Downloaded from rsta.royalsocietypublishing.org

PHILOSOPHICAL TRANSACTIONS OF THE ROYAL SOCIETY A MATHEMATICAL, PHYSICAL & ENGINEERING SCIENCES

An Investigation of Wind Structure in the Trades: Anegada 1953

H. Charnock, J. R. D. Francis and P. A. Sheppard

Phil. Trans. R. Soc. Lond. A 1956 **249**, 179-234
doi: 10.1098/rsta.1956.0019

Email alerting service

Receive free email alerts when new articles cite this article - sign up in the box at the top right-hand corner of the article or click **here**

To subscribe to *Phil. Trans. R. Soc. Lond. A* go to: **http://rsta.royalsocietypublishing.org/subscriptions**

This journal is © 1956 The Royal Society

Downloaded from rsta.royalsocietypublishing.org

AN INVESTIGATION OF WIND STRUCTURE IN THE TRADES: ANEGADA 1953

By H. CHARNOCK,* J. R. D. FRANCIS† and P. A. SHEPPARD†

(*Communicated by G. E. R. Deacon, F.R.S.—Received* 15 *November* 1955—*Revised* 15 *March* 1956—*Read* 7 *June* 1956)

CONTENTS

This paper describes an observational study of the mean and larger-scale turbulent structure of the wind in the lowest 1500 m of the North-East Trades. The observed motions are used both alone and in conjunction with the horizontal pressure field to deduce values of the vertical transport of momentum; the pattern of cumulus cloud convection is borne in mind throughout.

Sections 1 and 2 provide a brief survey of the background to the expedition and of the simplified equations by which the observations are interpreted.

Section 3 describes the site and observations in detail. 466 double-theodolite pilot-balloon soundings were made in the spring of 1953 from the small flat island of Anegada (18°N, 64°W). Soundings were made on 15 days over a 27-day period, balloons being released at intervals of 5 to 15 min. The balloons, rising at about 150 m/min, were observed every 20 s for 9 min, to obtain the three components of the motion in 50 m layers over the lowest 1350 m. Special observations of pressure were made in a network of neighbouring islands. The derivation of component air velocities and of the horizontal pressure gradient as a function of height is described in §4. Difficulty was experienced in obtaining the pressure field with requisite accuracy.

Surface observations of the weather in relation to the main aim of the study are discussed in §5. The mean angle between surface wind and isobar over the 15-day period was 13°, notably less than the climatological value of about 33°.

Section 6 discusses the properties of the mean horizontal motion for the whole period of observation. The easterly component of wind velocity was greatest at 350 m, and the wind veered with height through 24° in the first 1350 m. There was also a veer of geostrophic wind in this layer of about 13° so that some down-gradient motion remained at the top of the layer. It is shown that the mean values of the local and advective components of acceleration were negligible compared with others terms in the momentum balance.

Section 7 uses the wind profiles of §6 together with the mean horizontal pressure field to find the distribution of shearing stress with height, assuming that ageostrophic flow is balanced by internal friction. The mean stress in the direction of the surface wind varied from 0·41 dyn/cm² at the surface to −0·37 dyn/cm² at 1300 m. The former provides a coefficient of surface stress, based on the anemometer windspeed, $c = 1{\cdot}5 \times 10^{-3}$. The mean stress in the direction normal to the surface wind varied from zero (assumed) at the surface to 0·17 dyn/cm² at 200 m, and was small

* National Institute of Oceanography, Wormley, Surrey.
† Imperial College of Science, London.

The Royal Society is collaborating with JSTOR to digitize, preserve, and extend access to *Philosophical Transactions of the Royal Society of London. Series A, Mathematical and Physical Sciences.* www.jstor.org

Downloaded from rsta.royalsocietypublishing.org

above 800 m, but internal consistency is only obtained by assuming the horizontal gradient of temperature near the surface to be appreciably greater than the climatological value for the general area. The stresses and related gradients of mean motion imply eddy viscosities of order 10^5 cm^2/s throughout the layer.

Section 8 discusses the vertical profiles of daily mean wind, which are variable from day to day. It was not possible to analyze the profiles to find shearing forces because of uncertainty in the acceleration terms, and in the pressure field.

Section 9 is concerned with the analysis of fluctuations of wind at heights up to 1350 m, using averaging periods increasing from about 3 h up to the whole 27-day period. For none of these averaging periods was there equipartition of eddying energy in the three velocity components; $\overline{w'^2}$, the vertical intensity, was one to two orders of magnitude lower than $\overline{u'^2}$ and $\overline{v'^2}$, the horizontal intensities, the difference being greater the longer the averaging periods. The covariances $\overline{u'v'}$, $\overline{u'w'}$ and $\overline{v'w'}$ were also evaluated for various heights and averaging periods. $\overline{u'^2}$, $\overline{v'^2}$ and $\overline{u'v'}$ increased with averaging period and from their variation crude estimates are made of lag covariances which are equivalent to spectra. Values of $\overline{u'v'}$ for the larger components of the motion sampled were in fair agreement with those of early workers. $\overline{u'w'}$ and $\overline{v'w'}$ were in general less than $\overline{u'v'}$ and did not vary systematically with averaging period. The values for the smaller scale components of the motion sampled were in fair agreement with shearing stresses computed by the method of geostrophic departure (§7). The direction of the resultant of $\overline{u'w'}$ and $\overline{v'w'}$ agreed surprisingly well with the direction of the vertical shear vector of the mean wind velocity, the implied coefficient of eddy viscosity for the spectral range sampled again being about 10^5 cm^2/s over the whole range of height.

An appendix considers the effect of the island, about 30 km^2 in area, on the oceanic Trades; the land was strongly heated by the sun and a particular pattern of convective cloud was usually set up. The associated field of mean vertical motion, of the order of 10 cm/s, and the disturbance of the field of horizontal mean motion have been partly evaluated. It is found that the velocities measured on the upwind shore were fairly representative of those over the open ocean, even though slow steady rising and sinking motions were detected.

List of main symbols

x, y, z = rectangular co-ordinate axes with x-axis along theodolite base line PQ, z vertical.

X, Y, Z = rectangular co-ordinate axes with X-axis along direction of surface wind, Z vertical. Note that Z and z are interchangeable.

u, v, w = component wind velocities along x, y, z.

U, V = component wind velocities along X, Y.

U_J, V_J = component geostrophic wind velocities along X, Y.

U_0 = surface wind speed (0 to 50 m).

W = rate of ascent of balloon.

$\mathbf{q}$ = vector horizontal wind velocity.

$\mathbf{J}$ = vector geostrophic wind velocity.

θ = wind direction; suffix 0 for surface wind, J for surface geostrophic wind.

τ_{ik} = internal stress in i-direction for k-momentum, or conversely.

τ_0 = surface stress.

K_{ik} = eddy viscosity referred to a stress τ_{ik}.

l = Coriolis parameter $(2\omega \sin\phi) = 4{\cdot}73 \times 10^{-5}\,\mathrm{s}^{-1}$.

t = time.

ρ = air density, taken as $1{\cdot}2 \times 10^{-3}$ g/cm^3.

p = pressure.

T = temperature.

Downloaded from rsta.royalsocietypublishing.org

1. Introduction

The drag of the wind on the sea and the associated vertical transfer of momentum have received our attention for some time. Observations made near the Scilly Isles in January 1951 (Sheppard, Charnock & Francis 1952) suggested that the downwind shearing stress τ_{XZ} over the ocean in the westerlies did not vary significantly with height up to the maximum height at which observations were made, i.e. about 1 km. It was suggested that the shearing stress was due to turbulent transfer of momentum down a gradient of mean momentum, the gradient being due not only to friction but to a gradient of temperature in the horizontal —a thermal wind. The classical concept of a limited frictional surface layer was not valid, at least over the ocean. This extension of the usually accepted view was supported by independent climatological and other evidence.

From a practical viewpoint it seemed clear that estimates of τ_{XZ} (and in particular of the surface stress τ_0 which is so important in meteorology and oceanography) could not be made from measurements of mean wind only. This went some way toward explaining the discrepancy between observations of τ_0 made by oceanographic methods and by the method of geostrophic departure as used by Sutcliffe (1936) and others. Observations of the steady-state variation with height z of both wind and pressure gradient are required to determine $\partial\tau/\partial z$, where τ is the total stress in the horizontal. $\tau(z)$ can, of course, be deduced if τ is known at any particular level.

Making the plausible assumption that in the lower atmosphere the vertical flux of momentum is always down the gradient of mean horizontal momentum* it follows that

$$\tau_{XZ} = 0, \quad \text{where} \quad \partial U/\partial z = 0$$
$$\text{and } \tau_{YZ} = 0, \quad \text{where} \quad \partial V/\partial z = 0,$$

where U, V are components of mean wind velocity in horizontal co-ordinate directions X, Y (see list of symbols). Sheppard & Omar (1952) and Sheppard (1954), using this assumption together with routine synoptic data for the Trades (where the wind profile is adapted to the application of the above assumption) have found values for τ_0 which are not inconsistent with those found by other methods. The data used, however, were not sufficiently precise to provide definitive values; the work was regarded as a preliminary study, to be supported with an analysis of more accurate and more detailed observations.

This work, in conjunction with the observed fields of mean motion and mean temperature in the troposphere, has led Sheppard (1953, 1954) to a schematic model of the general circulation of the atmosphere which has several attractive features. It has also raised various problems regarding the mechanism of the turbulent transfer of momentum in deep layers of an atmosphere which is turbulent on all scales.

* At this stage of development of the subject, the validity of the assumption that the transfer of momentum is down the gradient of mean momentum is only to be tested against such observational evidence as may be found. Dryden (1948) suggests that in a simple two-dimensional boundary layer the flux of momentum is down the gradient of intensity of turbulence; in a pipe, however, the flux is necessarily down the gradient of mean motion. It is conceivable that, in the atmosphere, thermal or vapour buoyancy might provide a significant flux more or less independent of the gradient of mean motion, e.g. $\bar{u}\,\overline{\rho' w'}$ might be negative (downward flux) both below and above a turning point in the $\bar{u}$-profile. Such a flux is, however, probably only a significant part of the total vertical flux in regions of very light wind and therefore hardly significant climatologically. We shall present some evidence on this question in §9.

Downloaded from rsta.royalsocietypublishing.org

With this as a background, we decided to make an expedition to the Trades in order to undertake detailed and accurate measurements of the mean and medium-scale turbulent structure of the wind in the lowest 2 km and to relate the observed structure to the horizontal pressure field and the vertical transport of momentum. The wind structure was deduced from double theodolite observations of pilot balloons released from the Eastern Caribbean island of Anegada. This was a small flat island chosen so as to interfere as little as possible with the oceanic Trades. Nevertheless it was necessary to determine the modification produced by the island and in this we were fortunate enough to be able to work in close collaboration with a group from Woods Hole Oceanographic Institution. They were making meteorological measurements in and around trade cumuli using a Catalina aircraft equipped to make detailed measurements of temperature, wind and accelerations.

2. Theoretical framework of the observations

Our observations were made in the lowest 2 km of the North-East Trades of the Atlantic Ocean, in which there is a broad-scale, almost horizontal, flow with which are associated motions of smaller scale. The equations of horizontal acceleration can be written

$$\frac{\mathrm{d}U}{\mathrm{d}t}-l(V-V_J)=\frac{1}{\rho}\left(\frac{\partial\tau_{XX}}{\partial X}+\frac{\partial\tau_{XY}}{\partial Y}+\frac{\partial\tau_{XZ}}{\partial Z}\right), \tag{1}$$

$$\frac{\mathrm{d}V}{\mathrm{d}t}+l(U-U_J)=\frac{1}{\rho}\left(\frac{\partial\tau_{YX}}{\partial X}+\frac{\partial\tau_{YY}}{\partial Y}+\frac{\partial\tau_{YZ}}{\partial Z}\right). \tag{2}$$

Here ρ is the mean density of the air, the effect of fluctuations in density being neglected; U, V are component velocities of the broad-scale flow along horizontal rectangular co-ordinate axes X, Y (Z vertical); U_J, V_J are component geostrophic velocities computed from the broad-scale pressure gradient by

$$\rho l U_J=-\frac{\partial p}{\partial Y} \quad \text{and} \quad \rho l V_J=\frac{\partial p}{\partial X};$$

τ_{XX}, τ_{XY}, etc., are normal and tangential stresses arising from all fluid motions of smaller scale than the broad-scale flow.

There are good reasons for neglecting τ_{XX} and τ_{YY}; neither they nor their gradients exercise a direct influence on the flow. We also neglect for our purposes τ_{XY} and its gradients; the Trades have a rather uniform structure in the horizontal. Some empirical support for this assumption can be derived from an analysis of τ_{XY} arising from the large-scale flow components of the lower troposphere made by Starr & White (1952).

The broad-scale values of field quantities are found by taking an arithmetic mean over a selected period of observation.

Over the whole period of observations, i.e. 27 days, estimates (§ 6) show that both the local and advective components of the acceleration of mean motion are negligible, so that the equations (1) and (2) can be reduced to

$$\rho l(V-V_J)=-\frac{\partial\tau_{XZ}}{\partial z} \tag{3}$$

and

$$\rho l(U-U_J)=\frac{\partial\tau_{YZ}}{\partial z}. \tag{4}$$

Downloaded from rsta.royalsocietypublishing.org

We assume that τ_0, the resultant shearing stress at the surface, is in the direction of the mean wind over the lowest 50 m so that if the X-axis lies along this direction,

$$\tau_0 = \tau_{XZ}(z=0) \quad \text{and} \quad \tau_{YZ}(z=0) = 0.$$

Equations (3) and (4) can then be written

$$\tau_{XZ} = \tau_0 - \int_0^z \rho l(V - V_J)\,\mathrm{d}z, \tag{5}$$

$$\tau_{YZ} = \int_0^z \rho l(U - U_J)\,\mathrm{d}z. \tag{6}$$

If we now assume that $\tau_{XZ} = 0$, where $\partial U/\partial z = 0$,

and $\tau_{YZ} = 0$, where $\partial V/\partial z = 0$,

then from (5)

$$\tau_0 = \int_0^{z_1} \rho l(V - V_J)\,\mathrm{d}z \quad \text{if} \quad \partial U/\partial z = 0 \quad \text{at} \quad z = z_1 \tag{7}$$

and, from (6),

$$0 = \int_0^{z_2} \rho l(U - U_J)\,\mathrm{d}z \quad \text{if} \quad \partial V/\partial z = 0 \quad \text{at} \quad z = z_2. \tag{8}$$

$\tau_{XZ}(z)$ can therefore be calculated from (7) and (5) provided there is some level at which $\partial U/\partial z = 0$. It is this requirement which makes the method particularly suitable for use in the Trades, where there is commonly a maximum in the profile of U at a height less than 1 km. $\tau_{YZ}(z)$ can be calculated from (6), with (8) as a valuable constraint if there is a level at which $\partial V/\partial z = 0$. In § 7, mean values of $\tau_{XZ}(z)$ and $\tau_{YZ}(z)$ over the whole period of observations are found by these methods.

In § 8 we examine the daily mean profiles of U, V. Here $\mathrm{d}U/\mathrm{d}t$, $\mathrm{d}V/\mathrm{d}t$ can no longer be neglected, but we have not been able to estimate the components of the acceleration, temporal and advective, and of the geostrophic wind with sufficient accuracy to give an adequate description of the momentum balance on a daily basis.

Section 9 of the paper is concerned with statistics of departures from the mean wind, again defined as the arithmetical mean value of the observations over the whole working period or over shorter periods such as a day (about 7 h) or half a day (about 3 h). In making the computations described in this section it was convenient to use wind components u, v, w relative to rectangular co-ordinate axes x, y, z (z vertical) where the x-axis lies along the fixed base-line of the theodolite survey system. Thus the equations are formally the same as (1) and (2) with x, y, z replacing X, Y, Z, and $\bar{u}$, $\bar{v}$ replacing U, V, etc.

It is clear, from our results and from those of many other workers, that the effect of viscosity is negligible in comparison with the effect of small-scale fluid motions and we can write

$$\tau_{xx} = -\rho\overline{u''^2}, \quad \tau_{xz} = -\rho\overline{u''w''} \tag{9}$$

and similar expressions, where the double prime indicates the departure of the local, detailed flow from the mean flow. We are here assuming that the Reynolds meaning rules are approximately satisfied so that terms like $\overline{\bar{u}v''}$ can be neglected.

Our measurements are not sufficiently detailed to provide precise values of τ_{xx}, τ_{xz}, etc., but we have computed values of mean products like $\overline{u'^2}$ and $\overline{u'w'}$, etc., the single prime

Downloaded from rsta.royalsocietypublishing.org

indicating the departure of our observed velocities from the observed mean flow. These mean products can be regarded as the contributions to the complete products, i.e. $\overline{u''^2}$, $\overline{u''w''}$, etc., of motions on scales determined by our method of observation. The products $\overline{u'w'}$ and $\overline{v'w'}$ are of particular interest since they can be compared, after allowing for the change of axes, with τ_{XZ}/ρ and τ_{YZ}/ρ as determined from the mean motion in earlier sections.

The observations of the vertical motion of the balloons were sufficiently precise to provide a comprehensive set of data for the mean vertical motion $\overline{w}$ of the air as a function of the spatial co-ordinates, though there is some uncertainty in the velocity of balloons relative to the air. Nevertheless, these values of $\overline{w}$ and the distribution of horizontal wind velocity determined from ascents made from different release points enable us to give a partial description of the disturbance of the field of flow produced by the island. This description is contained in the Appendix.

3. The site and nature of the observations

3·1. *The site*

The ideal situation for a pilot-balloon investigation of oceanic Trade-wind air is an island so small and low that it does not give rise to island convection or topographical disturbances; yet large enough to give a sufficiently long base-line between two intervisible theodolite stations. It should also be surrounded by deep water. Such islands within the Trade-wind zone are rare and, except for some atolls in the Pacific, it seemed that the most suitable place was the island of Anegada (lat. 18° 45′ N, long. 64° 20′ W, local time meridian 60° W) in the Virgin Island group of the British West Indies.

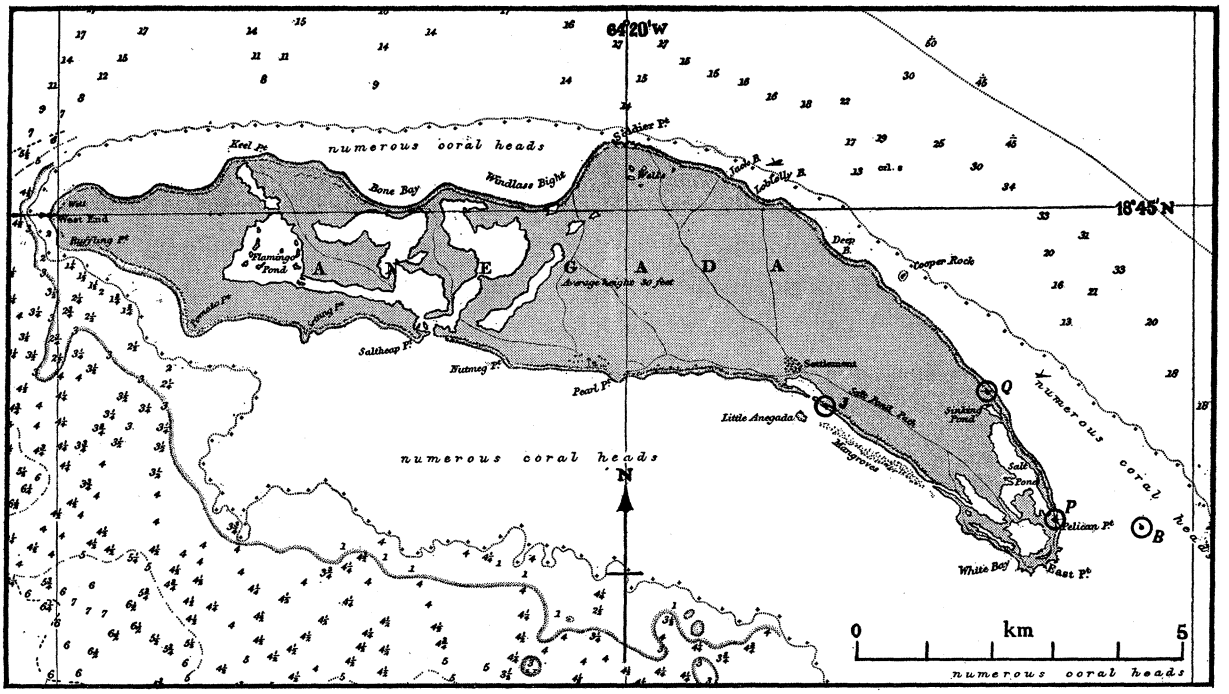

FIGURE 1. Portion of Admiralty chart 2008 showing Anegada and the surrounding sea. Base-line *PQ* used for primary series of double theodolite observations. Station *J* used for secondary series. *B* shows approximate position of boat for boat releases. (Chart reproduced by permission of the Hydrographer of the Navy and the Controller of Her Majesty's Stationery Office.)

Downloaded from rsta.royalsocietypublishing.org

This coral island (figures 1 and 2) is only about 10 m above sea level at its highest point and is about 12 km long, in a roughly south-east–north-west direction, and 3 km wide. On its north-east and east, i.e. windward, shores there is deep oceanic water for thousands of kilometres up to a coral reef about 300 m from the shore; there is water only 1 to 2 m deep to shoreward of the reef. The tidal range is only 20 cm with a pronounced diurnal component. The sea to leeward of the island is shallow for several kilometres, but access by sea on this side of the island is fairly easy.

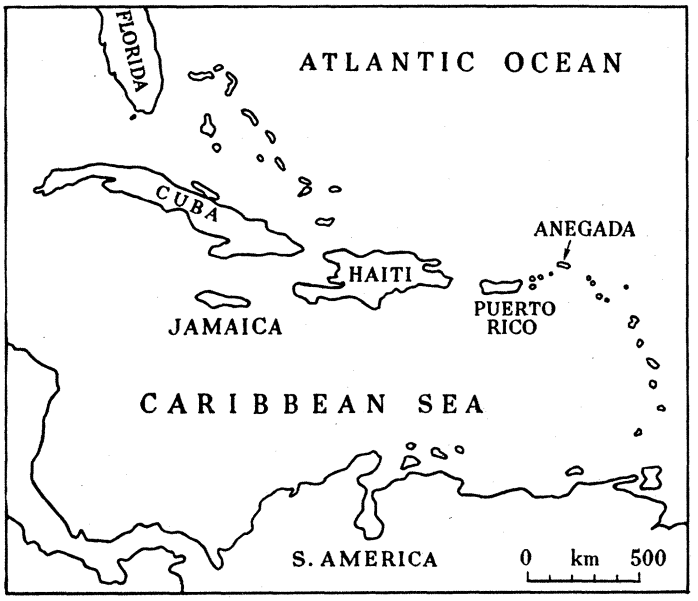

FIGURE 2. Location of Anegada relative to neighbouring land.

3·2. *The observational program*

Observations were made on Anegada in the period 12 March to 7 April 1953 and comprised:

(i) A primary series of balloon ascents, each observed from two theodolites simultaneously.

(ii) A secondary series of balloon ascents observed from one theodolite.

(iii) Barometric pressure.

(iv) Wind speed and direction by anemometer and wind-vane, air temperature and humidity near the surface.

(v) Visual observations of weather and some time-lapse photographs of clouds.

(vi) Profiles of mean wind speed up to about 4 m over the sea near station *P*. These profiles will be described and discussed in a separate paper.

In addition, special observations of barometric pressure and of air and sea temperature were taken for us in the Leeward and Virgin Islands by the U.S. Weather Bureau and the British Caribbean Meteorological Service.

3·3. *The primary series of ascents*

In this series, 466 pilot balloons were released in fifteen working days, each balloon being tracked simultaneously by two theodolites for 9 min (approx. 1·5 km height) whenever possible.

Downloaded from rsta.royalsocietypublishing.org

The base-line PQ (figure 1), 2340 m long in a 152 to 332° direction, was situated near the south-east end of the island; both theodolites being 15 m from the water's edge, and 4 m above sea level. The balloons, in a north-east wind, travelled nearly normal to the base-line, so that, in plan, the balloon and the two observing stations formed a well-conditioned triangle. On some days, however, the wind was well to south of east, so that balloons moved more nearly parallel to the base-line; to preserve the accuracy of location, the balloons were then released from a boat anchored just within the reef to the east of station P. The use of this additional release point also provided evidence on the effect of the island on the local wind field (see Appendix). The trajectories of the balloons in more or less homogeneous groups are shown relative to the island in figure A 1 (Appendix).

Red balloons, nominally 20 g in mass, were used for all soundings and, after weighing, were inflated to a standard horizontal diameter of 50 cm. This gave them a rate of ascent of about 150 m/min. They were released at about 10 min intervals from either P or Q or the boat station between 0930 and 1700 l.m.t., no night ascents being made. After release, they were observed in bearing and elevation every 20 s, i.e. at about 50 m intervals in height, from the theodolites at P and Q, synchronization to better than $\frac{1}{3}$ s being achieved by an audible time signal, controlled by a clock and relayed between stations by telephone.

The aim was to follow each balloon for 9 min, but some balloons were lost prematurely in cloud or for other reasons. The interval between soundings might then be shorter and was occasionally longer than 10 min. Some balloons which were followed in the two theodolites for 9 min were followed in one auxiliary theodolite for longer.

On the morning of the last working day, forty balloons were released at 5 min intervals and each was followed for 9 min, two theodolites being used at both P and Q. The effect of a higher frequency of sampling than the normal could thereby be investigated.

The pilot-balloon theodolites (M.O. Mk IV), which were occasionally interchanged between P and Q, were supported on concrete pillars, and the angles of bearing and elevation were read to 0·01°.

An essential feature of this series of observations was to locate the balloons with such precision and such frequency that horizontal and vertical components of displacement could be determined to about the nearest metre over layers not more than about 50 m deep. The required accuracy was in fact broadly achieved, as is indicated by the apparent difference in height of the balloon above the theodolite stations, using the elevation angles from each. The standard deviation of these differences, after allowing for small systematic errors in elevation angles of the theodolites, varied from about 0·5 to 0·8 m on individual ascents, and there was no evidence that the difference depended on height or distance within the range of variation of these quantities. The error in plan position should be much the same as the standard deviation of the height differences, so that the displacements, both in the horizontal and the vertical, can be considered correct to about ± 1 m. The corresponding component velocities of the balloon over 20 s intervals can therefore be considered correct to say ± 1 m/20 s or ± 5 cm/s. This error corresponds to errors in bearing and elevation of a few hundredths of a degree for the geometry of the system used and if we assume no error in timing.

Downloaded from rsta.royalsocietypublishing.org

Table 1 shows the duration for which balloons of the primary series were followed before being lost in cloud or haze, or by error of one observer. Thus 374 ascents were followed for 5 min or more, and these, together with thirteen ascents which were followed on 12 March, 24 March and 7 April for between 4 and 5 min, have been selected for further analysis, a total of 387 ascents. The other seventy-nine ascents have not been used in subsequent calculation.

TABLE 1. DISTRIBUTION OF THE TIMES FOR WHICH BALLOONS WERE FOLLOWED

time (min) for which balloons followed	<5	5 to $5\frac{2}{3}$	6 to $6\frac{2}{3}$	7 to $7\frac{2}{3}$	8 to $8\frac{2}{3}$	9	total
no. of balloons	92	32	25	31	29	257	466

The heights attained in the 387 analyzed ascents are given in table 2.

The rates of ascent, W, of the balloons during the soundings are given in table 3. Ascents covering the full 9 min are differentiated from the whole group of 387 analyzed ascents for reasons which appear in the Appendix.

The mean overall rate of ascent $\overline{W}$ has for simplicity been rounded off to 50 m/20 s in all subsequent analysis of grouped data, except in the Appendix. There was no significant correlation between the unfilled weights of the balloons and their rates of ascent over whole soundings; it is probable that variation in shape rather than weight was the main factor giving rise to the variations in the rate of ascent, vertical air motions apart (Ludlam 1953).

3·4. *The secondary series of ascents*

In this series balloons were released on a few days from a station J (figure 1) on the leeward coast of the island over the same periods as other balloons from the windward side, and were observed with a single theodolite. Weighing and filling were carried out according to the procedures for the primary series with some restrictions as to mass of balloons. The observations provide an important part of the information obtained on the effect of the island on the local wind field.

3·5. *Other observations*

Recording cup anemometers (M.O. cups Mk III, Bibby recorder) and wind-vanes were set up at stations Q and J, at the former site to provide a comparison with the wind velocity as deduced from the balloon flights over the first 50 m height, and at the latter site to provide information on the disturbance which the island created on the surface wind field.

4. THE COMPUTATIONS

4·1. *Primary series*

From each pair of observed bearings and elevations the plan co-ordinates x and y of the balloon were computed, and the height z found in two independent calculations. The zero for height was taken as the mean height of the two theodolites, i.e. 4 m above sea level, and the height of the balloon as the mean of the two computed values. No allowance was made for refraction or for the curvature of the earth. A constant correction to observed elevations was determined geometrically for each theodolite.

PHILOSOPHICAL TRANSACTIONS OF THE ROYAL SOCIETY A MATHEMATICAL, PHYSICAL & ENGINEERING SCIENCES
PHILOSOPHICAL TRANSACTIONS OF THE ROYAL SOCIETY A MATHEMATICAL, PHYSICAL & ENGINEERING SCIENCES

PHILOSOPHICAL TRANSACTIONS OF THE ROYAL SOCIETY A MATHEMATICAL, PHYSICAL & ENGINEERING SCIENCES
PHILOSOPHICAL TRANSACTIONS OF THE ROYAL SOCIETY A MATHEMATICAL, PHYSICAL & ENGINEERING SCIENCES

TABLE 2. DISTRIBUTION OF THE HEIGHTS UP TO WHICH BALLOONS WERE FOLLOWED

height (m)	700–800	800–900	900–1000	1000–1100	1100–1200	1200–1300	1300–1400	1400–1500	>1500
no. of ascents	25	32	16	18	35	88	120	46	7

TABLE 3. DISTRIBUTION OF THE OVERALL RATES OF ASCENT OF BALLOONS, ROUNDED OFF TO THE NEAREST 1·0 M/20 S

overall rate of ascent (m/20 s)	<40	40	41	42	43	44	45	46	47	48	49	50	51	52	53	54	55	56	57	58	59	>59	mean rate of ascent, $\overline{W}$	s.d.
no. of ascents (all 387 used)	1	0	3	3	12	15	16	26	34	43	47	46	41	27	24	12	19	8	0	5	1	4	49·5	3·7
no. of ascents which were followed for 9 min	—	—	2	1	10	9	12	19	19	30	36	32	25	22	14	9	11	4	0	2	—	—	49·2	3·4

Downloaded from rsta.royalsocietypublishing.org

Downloaded from rsta.royalsocietypublishing.org

The computations were carried out on Hollerith punched-card machines at the National Physical Laboratory, a tabulation of the following quantities being provided:

run no.	release point	time of release	time after release	x	Δx	y	Δy	z_1	z_2	$\lvert z_1-z_2\rvert$	$\bar{z}$	$\Delta\bar{z}$	mean of consecutive $\bar{z}$'s

where $\Delta x = x_n - x_{n-1}$ ($n = 1, 2, \ldots, 27$ for 9-min ascent),

$\Delta y = y_n - y_{n-1}$,

$z_1, z_2 =$ heights from respective theodolite elevations,

$\bar{z} = \frac{1}{2}(z_1 + z_2)$,

$\Delta\bar{z} = \bar{z}_n - \bar{z}_{n-1}$,

and the final column gives the height of the middle of the layer to which Δx, Δy, $\Delta\bar{z}$ refer. These tabulations are available (on application to the authors) to any reader who might wish to make use of them.

After the initial computations were completed the tabulations were scrutinized and anomalous values investigated. Some obvious errors in reading or in processing of the data were thereby located and could generally be corrected. An occasional gap in the tabulations, due to a missed reading or to one obviously in error, was made good by linear interpolation.

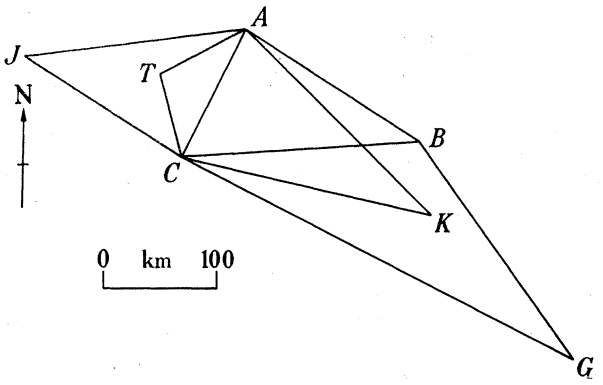

FIGURE 3. Mercator projection of network of pressure reporting stations used to find horizontal gradient of pressure. *J*, San Juan; *T*, St Thomas; *C*, St Croix; *A*, Anegada; *B*, St Barthelemy; *K*, St Kitts; *G*, Gaudeloupe. Gradients in triangles *JAC*, *JTA*, *ATC*, *ACB* all equally weighted 1·0; *ACK* weighted $\frac{2}{3}$; *CBG* weighted $\frac{1}{3}$.

4·2. *Secondary series*

These ascents, observed by a single theodolite only, were worked up using the Meteorological Office pilot-balloon slide rule, the rate of ascent being assumed to be 50 m/20 s.

4·3. *The pressure field*

The direction and magnitude of the horizontal pressure gradient $\nabla_h p$ at mean sea level in the vicinity of Anegada were determined from hourly readings of mercury barometers in the net of islands shown in figure 3, with, however, less frequent readings at Anegada itself. The barometers at stations *B*, *G*, *K* (figure 3) had recently been checked against a substandard, and those at *C*, *J*, *T* and the substandard were checked with the Anegada instrument at the conclusion of our observations. These comparisons were not, however, sufficient

PHILOSOPHICAL TRANSACTIONS OF THE ROYAL SOCIETY A MATHEMATICAL, PHYSICAL & ENGINEERING SCIENCES
PHILOSOPHICAL TRANSACTIONS OF THE ROYAL SOCIETY A MATHEMATICAL, PHYSICAL & ENGINEERING SCIENCES

TABLE 4. PRESSURE GRADIENT $|\nabla_h p|$ AND DIRECTION OF GEOSTROPHIC WIND IN TRIANGLES OF STATIONS NEAR ANEGADA

Gradients mb/(100 km). Directions from true north (deg).

triangle ...	*JAC*		*JTA*		*ATC*		*ACB*		*ACK*		*CBG*		weighted mean	
date	grad	dirn	grad	dirn	grad	dirn	grad	dirn	grad	dirn	grad	dirn	grad	dirn
12 Mar.	1·31	084	2·10	082½	1·13	107	1·24	088	1·61	068	0·59	093	1·38	085½
14	0·78	088½	1·66	084½	0·75	132½	0·78	090½	0·85	082	1·06	094	0·93	093
16	0·76	093	1·85	085½	0·83	147	0·80	086½	0·78	090½	0·33	091½	0·90	097
17	0·67	081	1·59	081	0·62	139	0·65	083½	0·56	124	0·00	—	0·75	094½
19	0·33	053½	0·41	059	0·28	059	0·16	100	0·16	100½	0·19	098	0·26	066½*
21 Mar.	0·60	091	0·70	089½	0·59	097	0·57	103	0·59	096	0·47	107½	0·60	095½
23	0·88	091	0·85	093	0·85	093	0·85	093	0·81	103½	0·37	106	0·83	094½
24	0·65	105	1·00	096	0·66	127½	0·65	105	0·64	112½	0·75	102	0·71	107½
26	0·40	121	0·41	120	0·40	124	0·41	128½	0·43	138½	0·52	117	0·42	125
27	0·48	121	0·32	009½	0·55	085	0·47	120	0·50	133	0·30	158½	0·35	104½†
28 Mar.	0·88	121	0·60	149	0·90	100½	0·88	120	0·87	121	0·69	134	0·79	121½
30	0·40	121	0·26	168	0·42	094	0·40	120½	0·41	126½	0·24	162½	0·34	124
1 Apr.	0·16	121	0·12	138½	0·16	108½	0·25	163	0·18	146½	0·32	133½	0·17	136
3	0·69	137	0·61	150½	0·66	126	0·66	110½	0·66	100½	0·48	120	0·60	127
4	0·26	166½	0·27	239	0·29	239	0·24	164	0·16	116½	0·28	141	0·22	155‡
7	0·15	173½	0·16	190½	0·13	166	0·19	180½	0·14	170½	0·20	154	0·16	175½
												overall mean gradient for all days	0·56	104

* Trough near. † Ignores *JTA*. ‡ Ignores *JTA*, *ATC* (trough near).

Downloaded from rsta.royalsocietypublishing.org

Downloaded from rsta.royalsocietypublishing.org

to provide values of $\nabla_h p$ of the required consistency. Consequently, station corrections were redetermined by drawing smooth isobars for the whole area for the whole period of observation. The departure of each station from the smoothed field value for that position was adopted as the station correction throughout the period. These corrections were all within $\pm 0{\cdot}1$ mb, except for Anegada ($-0{\cdot}3$ mb), where the barometer was of old design (accidents en route eliminated two Kew-pattern barometers) and was read less frequently. It is thought that small topographic effects on the pressure at some of the islands made the comparison of barometers of limited use for our purpose.

Mean values of $\nabla_h p$ for each working day were then found for each of the six triangles of stations shown in figure 3, and all six gradients were combined vectorially to give a mean $\nabla_h p$ for each day. The magnitudes of the gradients in the triangles were weighted as shown in figure 3 so as to obtain more representative gradients in the vicinity of Anegada.

The values of $\nabla_h p$ for each triangle and day and the weighted means are given in table 4. It will be seen that on most days the gradients from all six triangles were approximately the same in magnitude and direction. Only on days of slight gradient or on those days, e.g. 19 March, when the San Juan U.S.W.B. synoptic charts showed a markedly non-uniform pressure field in the area were the values of $\nabla_h p$ from the different triangles notably different. Nevertheless, it will be evident from table 4 that the weighted daily means in the final columns are subject to appreciable uncertainties, though it is impossible to ascribe limits. The overall mean values are necessarily more reliable, but again limits of accuracy can hardly be given.

4·4. *The temperature field and the variation of $\nabla_h p$ with height*

The solution by observation of equations (5), (6) and (7) requires the determination of $\nabla_h p$ as a function of height over the layer concerned. This was made from the field of surface temperature which over the sea should be adequate to provide the variation in $\nabla_h p$ over the lowest kilometre or so.

TABLE 5. CLIMATOLOGICAL TEMPERATURE GRADIENT NEAR ANEGADA (FROM M.O. 483)

	air-temperature gradient			sea-temperature gradient		
	°C/100 km	direction	no. of obs.	°C/100 km	direction	no. of obs.
March	0·25	195°	1007	0·22	191°	990
April	0·26	200°	999	0·23	193°	988

Mean gradient 0·24° C/100 km in direction 195°.

We found that the few surface observations made specially for us on fishing boats (arranged by the Meteorological Officer, U.S. Weather Bureau at San Juan) and those sent in to the Marine Division, Meteorological Office, gave conflicting evidence as to the small gradients that were present. We have therefore resorted to the climatological mean gradient for March and April (table 5), taken from the *Climatological Atlas of the Atlantic Ocean*, M.O. 483. The mean gradient of both air and sea temperature for the area within 200 km of Anegada has been used, but we shall show later that this is probably not typical of the gradients near Anegada, and that revised gradients must be inferred to explain certain features of the air motion.

Downloaded from rsta.royalsocietypublishing.org

5. Surface weather conditions

5·1. *The weather*

The weather during the 4 weeks over which our observations were made was presumably not untypical of the western end of a Trade wind 'cell' for the time of year. Trade cumuli with base at about 600 m height (as given by occasional observation from the Catalina aircraft) were present every day, but were much deeper on some days than on others, and were occasionally interrupted by larger-scale disturbances possessing much medium (As, Ac) and occasionally high (Ci) cloud. These disturbances mostly gave significant amounts of moderately heavy rain, as did many of the larger cumuli though the precipitation was then often distant. It was evident that the cumulus precipitation commonly fell

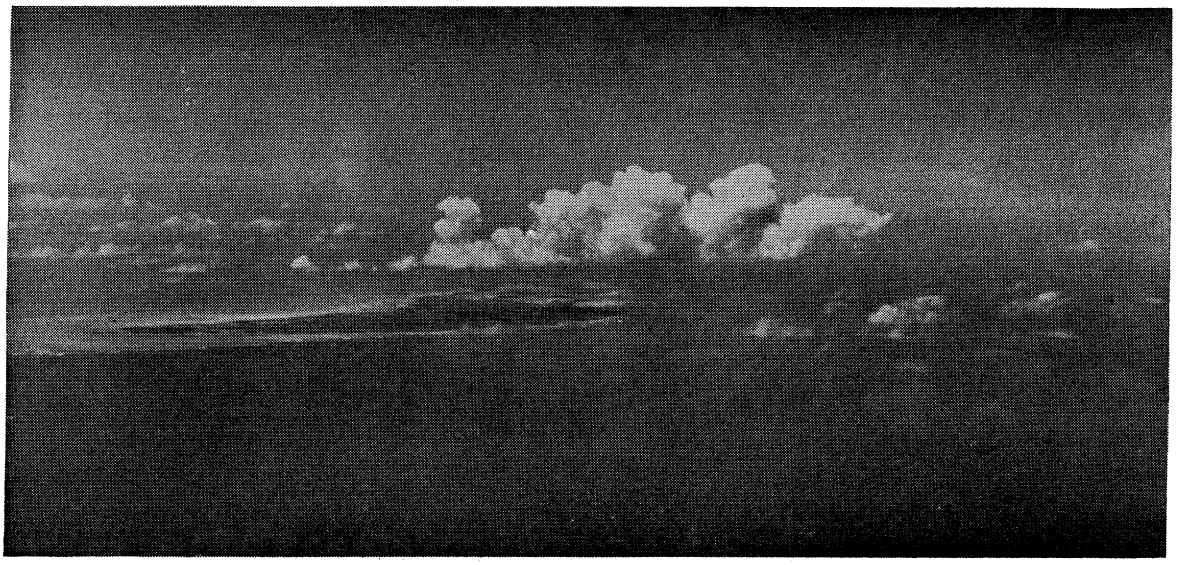

Figure 4. Aerial photograph of Anegada showing the island cumulus, the ring of nearly clear air around, and the Trade cumuli surrounding all. Photograph by K. McCasland.

from clouds whose tops were well below the 0° C isotherm, but some clouds were very great in depth, showing heavy anvil glaciation. Malkus & Ronne (1954) have described and analyzed one of these, on 1 April 1953, in some detail. Rain fell on or within sight of Anegada on 8 out of the 15 working days.

There was a notable diurnal variation in the weather over and immediately around Anegada. Towards 9 a.m. on a typical day a random variation of Trade cumuli gave way to a characteristic convection cloud pattern; the Trade cumuli were more or less suppressed over the island and a mile or two to seaward of it and were replaced by a single cumulus cloud 'street' whose upwind end was anchored to a position near the middle of the island and which extended for several miles more or less downwind but in a line which tended also to follow the banana-like shape of Anegada (see figure 4). The height of base and the depth of this cloud street were generally greater than those of the Trade cumuli and not infrequently the cloud street produced rain to leeward of the island when the Trade cumuli were insufficiently deep to give precipitation. The Anegada cumulus began to disperse at about 4 p.m. and by 7 p.m. the random distribution of Trade cumuli had become

Downloaded from rsta.royalsocietypublishing.org

re-established over the island. This diurnal variation in the pattern of convective cloud implies a corresponding variation in the incidence of vertical motion, on which evidence will be presented in the Appendix. It also implies that our sample of vertical and horizontal motion in the primary series of ascents may not be completely representative of the Trade wind air in the neighbourhood of Anegada. The balloons of the primary series rarely, if ever, disappeared into the Anegada cumulus.

The diurnal variation of air temperature at stations P and Q was about 1·5° C and at station J about 3·5° C. The diurnal variation in the temperature of the lagoon water was about 3 to 4° C.

5·2. *Surface wind; observed and geostrophic values*

We define the surface wind $\mathbf{U}_0$ as the mean wind over the first 20 s of balloon flight, i.e. approximately the lowest 50 m of the atmosphere. The relation of this wind to the wind observed by anemometer will be referred to below. Mean values of $\mathbf{U}_0$, from the primary series, and of the surface geostrophic wind $\mathbf{J}$, from the final columns of table 4, are given for each working day and for the whole working period in table 6. The ratio of U_0 to J and the difference in their directions are also given in this table, together with the climatological means and short remarks on the weather.

It will be seen that daily means of U_0 varied from 3·33 to 13·25 m/s and of J from 2·85 to 24·6 m/s, but that the lower and higher limits for U_0 did not occur on the same days as for J. The direction θ_0 of $\mathbf{U}_0$ varied between 058 and 146½°, the higher values occurring mainly towards the end of the working period. On some 'non-working' days the wind veered beyond the maximum in table 6, e.g. on 31 March when a disturbed rainy period took the wind occasionally into a westerly quarter. The lightness of these winds and the unsuitability of our base-line for them account in part for the absence of observations on these days.

The ratio U_0/J varies between 0·25 and 1·45 and the angular difference, $\theta_J - \theta_0$, between −11 and 80½°. The extremes in both these quantities may well be materially falsified by errors in the determination of $\nabla_h p$. The direction and the magnitude, relative to the true magnitude, of $\nabla_h p$ are most likely to have large errors when $|\nabla_h p|$ is small, and it is evident from table 6 that the extreme values of $\theta_J - \theta_0$ occur with the lower values of U_0 and J. There is, however, less evidence in this sense from the extremes of U_0/J. Moreover, if the value of $\theta_J - \theta_0 = 80\frac{1}{2}°$ (7 April) is excluded, there is a moderately well-defined linear relation between $\theta_J - \theta_0$ and U_0 and the negative values of $\theta_J - \theta_0$ for low values of U_0 might be interpreted (equation (3)) as a reversal of the normal sense of $\partial\tau_{XZ}/\partial z$ due to buoyancy. The effect of relatively large accelerations in the mean motion on some days is also perhaps not to be excluded in accounting for the more extreme values of U_0/J and $\theta_J - \theta_0$ (see § 8).

It will be observed from table 6 that the mean value of U_0 for all working days is a little higher than the long-term climatological value of U_0, and is also veered some 13° on the latter in spite of the exclusion of days with winds appreciably south of south-east from our working days. Our mean geostrophic wind J over all working days is also rather greater than the long-term climatological value and is backed 7° on the latter. The resulting difference of 20° in the angle $\theta_J - \theta_0$ of cross-isobar flow is rather disturbing, as the computed value of surface drag (equation (7)) is sensitive to this angle. The difference may be real, or it may arise from error in the U.S.W.B. normal maps on which Anegada lies close to the map edge, or from some undiscovered systematic error in our own determination of $\mathbf{J}$. It seems

Downloaded from rsta.royalsocietypublishing.org

unlikely that the mean wind direction obtained from M.O. 483 should have an error sufficient to account for the difference.

We shall bear the possibility in mind of error in $\theta_J - \theta_0$ when using it in § 7 for the determination of stress.

TABLE 6. DAILY AND PERIOD-MEAN SURFACE AND GEOSTROPHIC WINDS

* Denotes maximum value; † denotes minimum value.

period over which ascents were made (l.m.t.)	date	no. of ascents on which $\mathbf{U}_0$ based	$\mathbf{U}_0$ speed, U_0 (m/s)	$\mathbf{U}_0$ dirn, θ_0 (deg.)	$\mathbf{J}$ speed, J (m/s)	$\mathbf{J}$ dirn, θ_J (deg.)	U_0/J	$\theta_J - \theta_0$ (deg.)	remarks
1000 to 1652	12 Mar.	13	11·30	058	24·6*	085½	0·46	27½	showers
0925 to 1643	14	18	10·15	076	16·6	093	0·61	17	
0945 to 1656	16	33	6·35	064	16·0	097	0·40	33	shower early
0929 to 1628	17	28	3·33†	090	13·4	094½	0·25	4½	
0922 to 1632	19	33	4·87	077½	4·6	066½	1·06	−11	trough near; showers in distance
0925 to 1632	21	30	5·30	094½	10·5	095½	0·51	1	showers
0935 to 1643	23	32	8·35	071½	14·8	094½	0·56	23	
0948 to 1648	24	26	13·25*	082	12·6	107½	1·05	25½	rain
0918 to 1647	26	30	7·55	112	7·5	125	1·01	13	
1035 to 1637	28	29	6·35	118½	14·0	121½	0·45	3	shower early
0948 to 1333	30	12	8·07	126½	6·1	124	1·32	− 2½	shower early
1128 to 1642	1 Apr.	13	3·35	146½	3·0	136	1·12	−10½	
1134 to 1620	3	17	4·70	135	10·7	127	0·44	− 8	
1059 to 1643	4	20	4·70	120½	3·9	155	1·21	24½	trough near; showers in distance
0913 to 1610	7	44	4·15	095	2·85†	175½	1·45	80½	
mean of all working days		—	6·10	091	10·1	104	0·60	13	
mean for March and April 1953		—	—	—	10·7 (*a*)	100 (*a*)	—	—	
climatological mean March and April		—	4·72 (*b*)	078 (*b*)	8·9 (*c*)	111 (*c*)	0·53	33	

(*a*) From U.S. Weather Bureau Climatological Data National Summary, 1953.
(*b*) From Meteorological Office Monthly Charts of Atlantic, M.O.483, 1948.
(*c*) From U.S. Weather Bureau Normal Weather Maps, Northern Hemisphere, *U.S.W.B. Tech. Pap.* no. 21, October 1952.

5·3. *The relation of the wind at anemometer level to the mean wind over the first* 50 *m*

The cup anemometer at station Q was fixed at a height of 7 m above the ground, and was arranged to give average wind speeds over 3 min intervals on a Bibby recorder. The accuracy of measuring the record for a 3 min period is about $\pm 0{\cdot}25$ m/s. Owing to mechanical troubles with the recorder, reliable records over extended periods were only obtained on three working days, and it is from these records that a comparison has been made with the mean wind over the first 50 m from the balloon flights made during the same periods. The results of the comparison are given in table 7.

It will be seen that the ratio of the mean wind speed over the first 50 m to that at 7 m is consistently greater than unity, as expected, but that it is subject to appreciable variation. Some of this variation is doubtless due to the inadequacy of sampling by balloons—20 s flights made at 10 min or so intervals—relative to the continuous sampling by the anemometer. The mean value of the ratio, 1·16, is, however, probably representative to within a small percentage. Since station Q was within a few metres of the shore, the application of this ratio (actually its inverse) to the 'surface' wind U_0 as measured by balloon is likely to give reasonably representative values of wind at anemometer level over the sea immediately upwind of station Q.

Downloaded from rsta.royalsocietypublishing.org

The mean deviations of wind speed about the 'half-day' means of table 7 are about the same for the two measures of mean wind speed. The shorter period of sample for individual values by balloon, 20 s against 3 min for the anemometer, probably offsets the lack of continuity in the balloon sampling.

TABLE 7. COMPARISON OF THE MEAN WIND SPEED U_0 (M/S) IN LOWEST 50 M BY BALLOON, WITH THE ANEMOMETER WIND SPEED U_a AT 7 M

	balloons: mean speed over 50 m			anemometer: mean speed at 7 m			
date and time	no. of ascents	U_0	mean devn	no. of 3 min periods	U_a	mean devn	U_0/U_a
26 Mar. a.m.	18	7·97	±0·44	53	7·15	±0·5	1·11
p.m.	18	7·15	±0·39	64	6·40	±0·3	1·12
28 Mar. a.m.	10	7·25	±0·52	29	5·86	±0·4	1·24
p.m.	19	5·95	±0·38	65	5·10	±0·4	1·17
3 Apr. a.m.	10	5·51	±0·37	34	4·52	±0·6	1·22
p.m.	9	4·11	±0·23	38	3·76	±0·4	1·10
						mean value	1·16

6. THE PROPERTIES OF THE PERIOD-MEAN HORIZONTAL MOTION

6·1. *The vertical profiles of the period-mean horizontal motion*

The vertical profiles of the mean horizontal components of wind velocity U and V, along and normal to the mean surface wind direction respectively, for the ascents of the primary series over the whole working period (15 days of observations) are given in figure 5. Each point is the mean over a layer of average depth 50 m and the velocity is ascribed to the middle of the layer.

The characteristic maximum of the total wind speed, or of its easterly component, for Trade wind air is clearly shown in figure 5 in the maximum of the closely related U at a height z $(= z_1)$ of 350 m. This maximum is much more strongly defined on most of the daily mean profiles to be shown later, but the variable height at which it occurs inevitably smooths the period-mean profile.

The profile of V, drawn reversed in figure 5, shows a numerical increase of V with height up to about 900 m above which it is sensibly constant. There was a considerable day-to-day variation in the form of this profile, and it is not to be inferred that figure 5 necessarily shows a representative form of the climatic mean. The constancy of V above 900 m $(= z_2)$ in the present series is, however, a fortunate circumstance in that it allows application of the constraint expressed by equation (8).

It seems unlikely that the slight inhomogeneity of data above about 700 m has resulted in the profiles of figure 5 being unrepresentative in the upper levels.

In a given field of surface pressure, the wind at any height is determined, in the steady state (cf. equations (3), (4)), by the horizontal temperature gradient and by the vertical flux of horizontal momentum. The equations can be solved for U and V by assuming a realistic relation between the shearing stress and the wind distribution. Ellison (1956), in particular, has given a solution in which the fundamental role of the thermal wind is

Downloaded from rsta.royalsocietypublishing.org

recognized. We shall not pursue the matter here, regarding our observational data of later sections as a basis for future work along lines similar to those of Ellison.

The vertical profile of mean wind direction is given in figure 6. It does not have the attributes of the profile for a barotropic friction layer. A tentative assessment of the profile

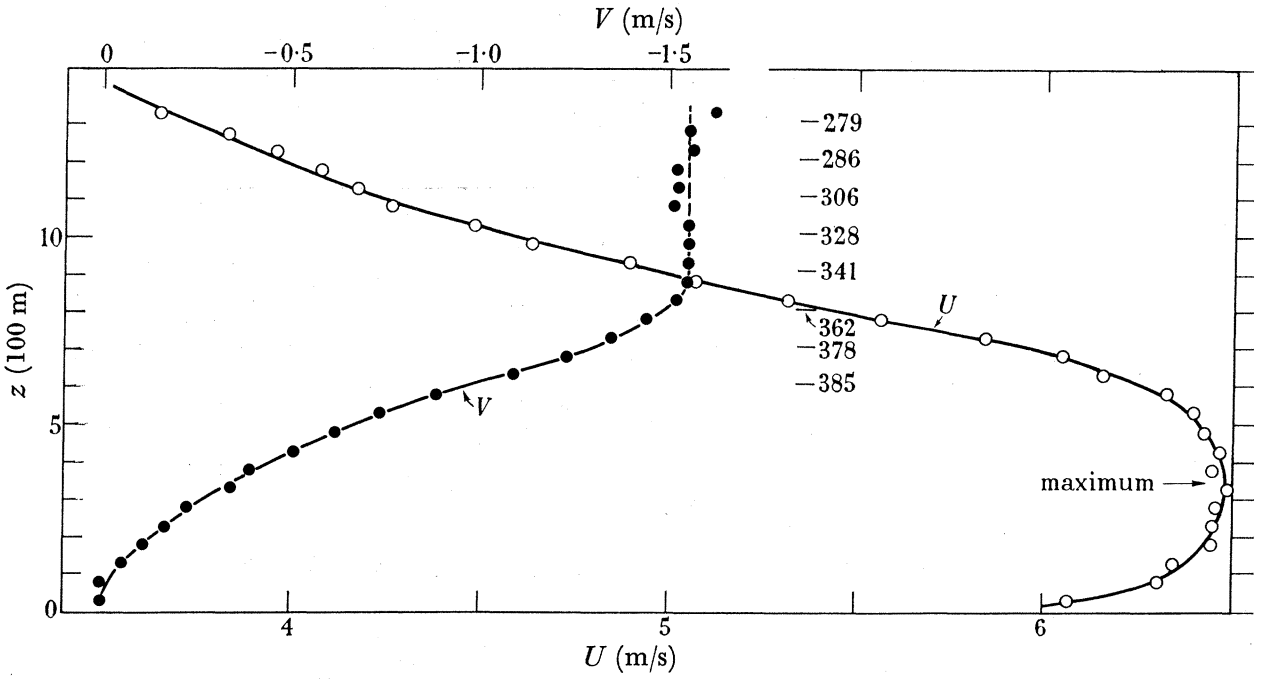

FIGURE 5. The vertical profiles of the period-mean horizontal motion. Data for all 15 working days. Number of ascents to each level given above 600 m.

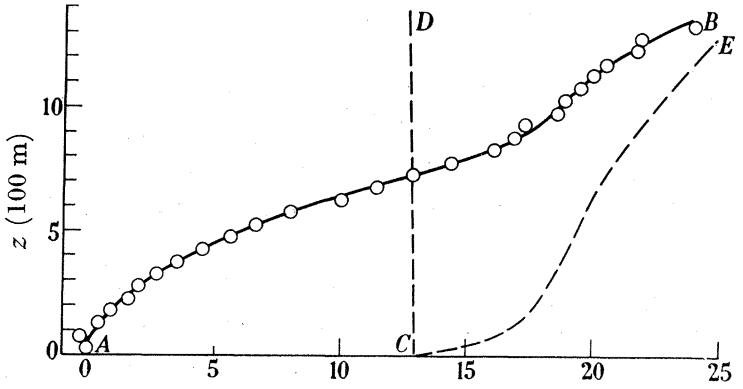

FIGURE 6. Period-mean profiles of observed and geostrophic wind directions. *AB* refers to the observed wind direction; *CD* to the geostrophic wind direction assuming the climatological temperature gradient; and *CE* to the geostrophic wind direction indicated in §7·2.

of mean geostrophic wind direction is included in figure 6 for comparison, but discussion of this profile will be given later. The veer with height of the observed wind is about the same as that found in the west-central Pacific Trade over a 16-month period by Sheppard & Omar (1952), but it is materially greater than that found in the eastern Pacific Trade between July and October 1945 by Riehl *et al.* (1951).

Downloaded from rsta.royalsocietypublishing.org

6·2. *The acceleration of the period-mean motion*

Since the use of equations (5) to (8), in conjunction with the profiles of figure 5, demands that the accelerations in the mean motion be negligible, it is appropriate to attempt some estimate of them.

If the motion is purely horizontal with mean velocity $\mathbf{q}$ the acceleration $\mathrm{d}\mathbf{q}/\mathrm{d}t$ may be written

$$\frac{\mathrm{d}\mathbf{q}}{\mathrm{d}t} = \mathbf{s}\left(\frac{\partial q}{\partial t} + q\frac{\partial q}{\partial s}\right) + \mathbf{n}\left(\frac{q^2}{r} + q\frac{\partial \theta}{\partial t}\right),$$

where $\mathbf{s}, \mathbf{n}$ are unit vectors along and normal to the motion at the point considered. θ is the wind direction and r is the radius of curvature of the streamline through the point. We have estimated the terms on the right-hand side of this expression and consider first the terms in t.

Because our soundings were effectively confined to the interval 0900 to 1700 l.m.t. it is appropriate to examine them for diurnal variation in speed and direction over the main part of the working day. The analysis was confined to the surface wind for which no clear diurnal variation was found. It appeared that $\partial q/\partial t$ was at most $0{\cdot}4\,\mathrm{m\,s^{-1}}/4\,\mathrm{h}$ and $q\partial\theta/\partial t$ at most $6\,\mathrm{m\,s^{-1}} \times 3^\circ/4\,\mathrm{h}$, or in units to be used later of force per unit volume of air, 0·03 and $0{\cdot}02\,\mathrm{dyn\,cm^{-2}}/100\,\mathrm{m}$ respectively. As will be shown later these forces are small compared with those retained in equations (3) and (4) which are the basis of equations (5) to (8). The terms in t arising from the change in q and θ over the whole period of investigation are of course much smaller.

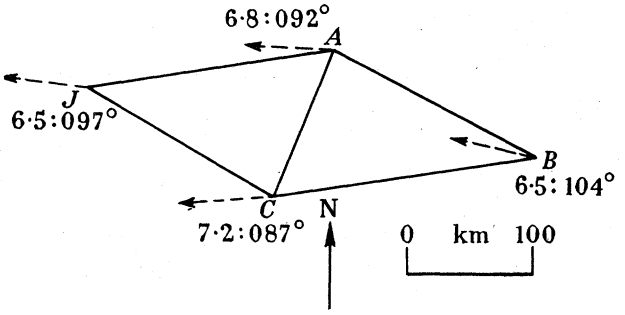

FIGURE 7. The period-mean wind velocities at four islands including Anegada. Averages over all working days from two ascents per day, for winds at 330 and 660 m. Vectors to scale. Speed, m/s: direction, degrees.

An attempt to estimate the other two terms in the expression for the acceleration has been made by analyzing the routine pilot-balloon ascents made at 0900 and 1500 l.m.t. by the respective meteorological authorities at San Juan, St Croix and St Barthelemy on each of our working days. The surface winds at these stations are probably unrepresentative for our purpose, because the islands are large or hilly. The wind speed and directions at 330 and 660 m, which are perhaps more representative, have therefore been averaged together over the whole period to form for each station a single period-mean wind speed and direction, for the combined heights. A similar averaging has been done for the Anegada ascents nearest 0900 and 1500. The mean values are shown plotted in their relative geographical positions in figure 7, whence it appears that the gradients of velocity are small, both along

Downloaded from rsta.royalsocietypublishing.org

the mean direction of motion 095° and also normal to it. The term $q\partial q/\partial s$ is perhaps about $7\,\mathrm{m/s} \times 0{\cdot}1\,\mathrm{m\,s^{-1}}/100\,\mathrm{km}$, i.e. force per unit volume $\rho q\partial q/\partial s = 0{\cdot}008\,\mathrm{dyn\,cm^{-2}}/100\,\mathrm{m}$, and, since the streamlines might swing through about 5°, $\rho q^2/r$ may be about $0{\cdot}01\,\mathrm{dyn\,cm^{-2}}/100\,\mathrm{m}$. Again they are both small compared with the terms retained in equations (3) and (4).

The acceleration arising from mean vertical motion, which is not included in the above expression of the acceleration, cannot be estimated from our observations since we have no measurements of the relevant mean value of vertical motion. The vertical gradient of U (see figure 5), from 600 to 1300 m height, is about $-4\,\mathrm{m\,s^{-1}/km}$ and of V, from 0 to 800 m height, is about $-2\,\mathrm{m\,s^{-1}/km}$. Taking the former as the extreme, a mean vertical motion of $\overline{w} = 2\,\mathrm{cm/s}$ would be required to provide a force per unit volume of air ($\rho\overline{w}\partial U/\partial z$) of $0{\cdot}1\,\mathrm{dyn\,cm^{-2}}/100\,\mathrm{m}$, which is the order of the terms in equations (3) and (4). Indirect evidence from other sources, e.g. Riehl *et al.* (1951), suggests that the mean vertical motion in the Trades is probably two orders of magnitude down on this value, so that we are justified in neglecting it in our budget of mean momentum in the lowest 2 km of the atmosphere. The mean vertical motions of the air produced over and immediately around the island site by solar heating (see Appendix) are not considered to be significant in this connexion. To a first approximation at least, the acceleration arising from this vertical motion is balanced by the local advective acceleration, as may be inferred from the results given in the Appendix. The local advective acceleration is also neglected in equations (3) and (4).

7. Shearing stress and its variation with height

7·1. *The period-mean values of stresses*

The period-mean profiles of wind are now used with the pressure field to obtain the stresses τ_{XZ} and τ_{YZ} at 100 m vertical intervals, following the theoretical analysis of § 2. A knowledge is required of the components of the geostrophic wind along the surface wind direction, U_J, and normal to it, V_J, at all heights in the layer investigated. The analysis is first carried out assuming that the large-scale surface temperature gradient given in table 5 is adequate to provide the variation in U_J and V_J in the first 1350 m depth of air. We have, to a sufficient approximation,

$$-\frac{\partial U_J}{\partial Z} = \frac{g}{lT}\frac{\partial T}{\partial Y} \quad \text{and} \quad \frac{\partial V_J}{\partial Z} = \frac{g}{lT}\frac{\partial T}{\partial X},$$

where $g/lT = 0{\cdot}67\,\mathrm{cm\,s^{-1}\,°C^{-1}}$ for $T = 300°\,\mathrm{K}$. The climatological value of $\nabla_h T$ being $0{\cdot}24°\,\mathrm{C}/100\,\mathrm{km}$ in a direction 195°, these equations give values referred to the surface wind direction (091°) of

$$\frac{\partial U_J}{\partial Z} = 0{\cdot}16\,\mathrm{m\,s^{-1}}/100\,\mathrm{m}, \quad \frac{\partial V_J}{\partial Z} = 0{\cdot}04\,\mathrm{m\,s^{-1}}/100\,\mathrm{m}.$$

The integrals of equations (5) to (7) have been evaluated by a step-by-step method over 100 m layers (50 m layers in the first 100 m), U and V being taken from the smoothed profiles of figure 5 and U_J, V_J from § 4·3 and the previous paragraph. The height Z_1 for maximum U is taken as 350 m. The resulting values of τ_0, τ_{XZ} and τ_{YZ} are given in table 8. Here the values of τ_{YZ} have not been subject to the constraint provided by equation (8);

Downloaded from rsta.royalsocietypublishing.org

they will be revised later. Table 8 also contains the eddy viscosities K_{XZ}, K_{YZ} at different levels, computed by means of the relations

$$K_{XZ} = \tau_{XZ} \Big/ \rho \frac{\Delta U}{\Delta Z} \quad \text{and} \quad K_{YZ} = \tau_{YZ} \Big/ \rho \frac{\Delta V}{\Delta Z},$$

where ΔU and ΔV are the changes of U and V in a layer $\Delta Z = 100$ m thick, centred on the level Z.

TABLE 8. STRESSES AND EDDY VISCOSITIES FROM PERIOD-MEAN WIND PROFILES, SURFACE PRESSURE-GRADIENT AND CLIMATOLOGICAL TEMPERATURE GRADIENT (CF. TABLE 9)

z (m)	τ_{XZ} (dyn/cm²)	K_{XZ} (10^5 cm²/s)	τ_{YZ} (dyn/cm²)	K_{YZ} (10^5 cm²/s)
0	$0{\cdot}41 = \tau_0$	—	0	—
50	0·34	0·55	0·11	4·4
100	0·28	1·17	0·20	2·08
200	0·16	1·92	0·38	2·89
300	0·05	2·17	0·61	3·15
400	−0·05	1·0	0·76	3·18
500	−0·13	1·22	0·91	3·04
600	−0·20	0·69	1·06	2·60
700	−0·25	0·51	1·21	3·88
800	−0·28	0·54	1·38	8·8
900	−0·30	0·63	1·56	—
1000	−0·32	0·69	1·76	—
1100	−0·34	0·91	—	—
1200	−0·35	1·29	—	—
1300	−0·37	1·59	—	—

Before discussing the contents of table 8 in detail it is worth pointing out that the changes in τ_{XZ}, τ_{YZ} between levels 100 m apart are mainly of order 0·1 dyn/cm², that is, are large compared with accelerations of the mean motion as inferred above. We have some confidence therefore in regarding equations (3) and (4) as adequately descriptive of the balance of mean momentum in the lower 2 km of the Trades. Although we shall see below that table 8 stands in need of some revision, the nature of the balance is unaffected.

The mean value of the surface stress τ_0 ($= \tau_{XZ}$ at $Z = 0$) is seen to be 0·41 dyn/cm². The shear-stress coefficient c ($\equiv \tau_0/\rho U_0^2$) is then, with $U_0 = 6{\cdot}07$ m/s and $\rho = 1{\cdot}2 \times 10^{-3}$ g/cm³, equal to $0{\cdot}92 \times 10^{-3}$. It is, however, usual to evaluate the shear-stresss coefficient for a 'surface' wind measured at the common anemometer height of about 10 m. The ratio of mean wind speed over 50 m height and at our anemometer level was found (§ 5·3) to be 1·16, giving the revised value

$$c = 1{\cdot}24 \times 10^{-3} \quad \text{for} \quad U_a = 5{\cdot}23 \text{ m/s}.$$

This value of c agrees quite closely with previous estimates by the same method by Sheppard & Omar (1952) and Sheppard (1954) using cruder, though more numerous, data.

The variation in τ_{XZ} with height agrees in form and approximately in magnitude with that to be inferred from Riehl *et al.* (1951) for the eastern Pacific Trades and as given by Sheppard (1954) from climatological data for the Atlantic Trades. The increase of $-\tau_{XZ}$ with height above about 700 m is, however, somewhat less than suggested by the papers cited.

Downloaded from rsta.royalsocietypublishing.org

The eddy viscosity K_{XZ} increases with height up to about 100 m, then remains of the order of $10^5\,\mathrm{cm^2/s}$ with some suggestion of a minimum in the middle of the layer investigated. Since the mean horizontal motion measured above cloud base (600 m or so) is not unlikely to be representative of both clear and cloudy air, though the balloons were observed only in clear air, the suggested rise in K_{XZ} above 800 m may well reflect the action of the clouds in promoting momentum transfer.

Table 8 shows an unacceptably rapid increase of τ_{YZ} with height, and this is reflected in values of K_{YZ} which are systematically larger than those of K_{XZ}. The computations of τ_{YZ} have not, however, been subjected to the constraint imposed by equation (8) and the effect of this will now be examined.

7·2. *Revised values of stress using revised values of the variation of geostrophic wind with height*

The values of τ_0 and $\tau_{XZ}(Z)$ are not greatly sensitive to the variation of V_J with height (equations (5) and (7)), within the possible limits of this variation; they depend essentially upon the observed profiles of U and V and on the surface value of V_J. It is otherwise with τ_{YZ} which is quite sensitive to the variation of U_J with height within the wider possible limits of its variation—wider, because $\nabla_h T$ is nearly meridional and U_J nearly zonal. Fortunately (see figure 5) we found that V remained practically constant above about 850 m. We can therefore use equation (8) which prescribes the value zero to τ_{YZ} where $\partial V/\partial Z = 0$. That is, we can determine τ_{YZ} above 850 m on evidence quite distinct from that used for its evaluation by means of equation (6).

In applying the constraint we shall assume that our value of U_J at the surface is correct so that only the variation of U_J with height is in question. This implies that we should be able to draw a curve of U_J against height with a fixed lower point and such that it intersects the U profile to give equal areas between the two curves below the level of 850 m and with $U = U_J$ above.

The line *LHNS* of figure 8 shows our estimate of $U_J(Z)$ based on these considerations. (To have drawn the curve of U_J to meet the curve of U at 850 m and to coincide with it above that level would have involved a significant inflexion in the U_J curve at a lower level, implying a non-monotonic variation of $\partial T/\partial Y$ with height. Such a variation seemed unlikely and the curves of U and U_J are shown therefore to meet at a somewhat higher level than 850 m.) In figure 8 the area $MRHN$ = area KHL, where MN is drawn at the level 850 m, so that $\tau_{YZ} = 0$ at 850 m. The area SMN therefore indicates a small stress τ_{YZ} at $Z = 1100$ m (the level of S) which, for what it is worth, is not inconsistent with the slight reversal of slope of the $V(Z)$ curve between 1000 m and 1150 m (figure 5).

The revised form of the $U_J(Z)$ relation implies much larger values of $\partial T/\partial Y$ in the first 300 m or so than are obtained from the climatological charts. The latter give a value of $0{\cdot}23^\circ\,\mathrm{C}/100\,\mathrm{km}$ for $\partial T/\partial Y$, but figure 8 shows values from $3{\cdot}2^\circ\,\mathrm{C}/100\,\mathrm{km}$ at the surface to $0{\cdot}34^\circ\,\mathrm{C}/100\,\mathrm{km}$ at 1100 m. There is no sound internal evidence for revising the climatological chart value of $\partial T/\partial X$ or the corresponding variation of V_J with height, so that the resultant horizontal temperature gradient $\nabla_h T$ obtained by combining this value of $\partial T/\partial X$ with the revised values of $\partial T/\partial Y$ is $3{\cdot}2^\circ\,\mathrm{C}/100\,\mathrm{km}$ at 182° for the surface and $0{\cdot}34^\circ\,\mathrm{C}/100\,\mathrm{km}$ at 191° for $Z = 1100$ m. The latter is reasonably near the climatological chart value ($0{\cdot}24^\circ\,\mathrm{C}/100\,\mathrm{km}$ at 195°), whereas a much enhanced surface value of $\nabla_h T$ is plausible

Downloaded from rsta.royalsocietypublishing.org

because of the rather sudden transition from deep ocean water north-east of Anegada to the much shallower water around it and to the west. The climatological charts will smooth the effect of this transition. The actual value of $|\nabla_h T|$ here derived for the surface may, however, be excessive, and one must then infer some overestimate of U_J at the surface. The consequence of such an overestimate will be discussed below.

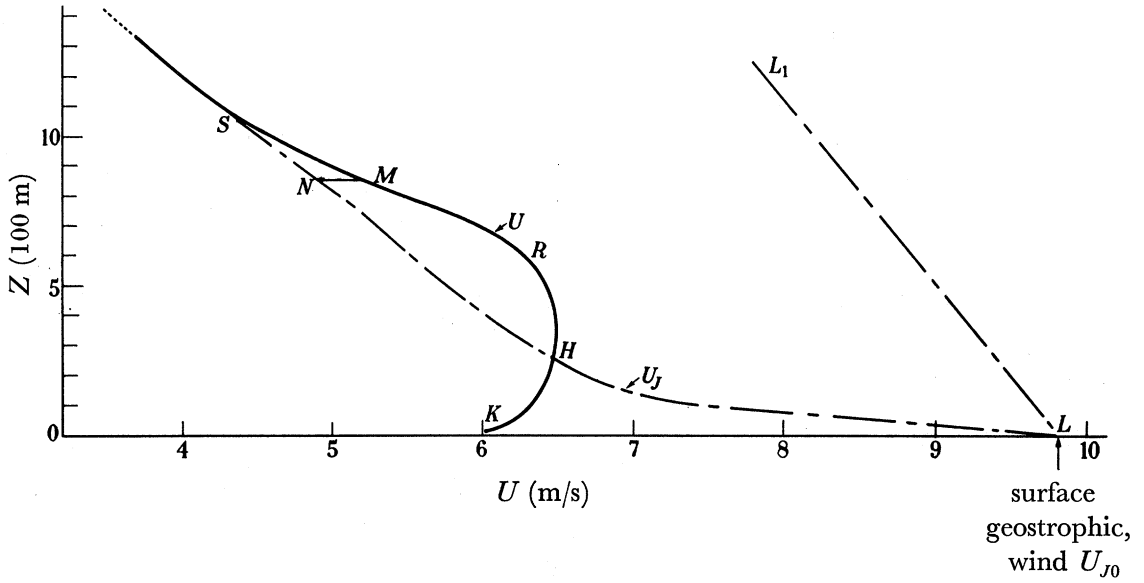

FIGURE 8. Vertical profiles of period-mean values of U and U_J. *KHRMS* is the observed wind component U. *LHNS* is the revised geostrophic component U_J, §7·2, drawn to give $\tau_{YZ}=0$ at 850 m, where $\partial V/\partial Z=0$. LL_1 is the geostrophic component drawn with a slope corresponding to the climatological temperature gradient, $\partial T/\partial Y$, §7·1. The slope of the lowest part of *LHNS* corresponds to a temperature gradient of 3·2° C/100 km. The slope above *S* corresponds to a temperature gradient of 0·34° C/100 km.

The revision of $U_J(Z)$ leads also to a change in the direction of $\mathbf{J}(Z)$. In the absence of further information on the other geostrophic component $V_J(Z)$, we have combined the revised $U_J(Z)$ of figure 8 with the climatological value of $V_J(Z)$ used in table 8, to give a revised geostrophic direction. It is shown in figure 6, together with the observed wind direction and the geostrophic wind direction assumed in table 8. It will be seen that the geostrophic wind direction is now veered on the observed wind direction at all levels but less aloft; a more convincing behaviour than that of the climatological geostrophic wind which is first veered, then backed on the observed wind.

The revised values of $U_J(Z)$ shown by the line *LHNS* in figure 8 lead to revised values of τ_{YZ} and K_{YZ} given in table 9.

The pattern of $\tau_{YZ}(Z)$ is now necessarily more realistic than that given in table 8, though the rather rapid increase of τ_{YZ} in the first 100 m compared with the variation from 100 to 300 m suggests that the surface value of U_J is indeed somewhat overestimated. We note also that the revised values of K_{YZ} are now more closely in agreement with those of K_{XZ} in table 8, but that there is an immediate decrease of K_{YZ} with height from the surface, itself indicative of too high a value of τ_{YZ} ($Z=100$ m) and so of U_J ($Z=0$). Note also that the values of K_{YZ} at about 800 m are low relative both to the lower levels and to K_{XZ}. The uncertainty in

Downloaded from rsta.royalsocietypublishing.org

estimation of K_{YZ} owing to the small gradient of V near 800 m is not wholly responsible for this latter feature.

The analysis of this and the previous section leads to the conclusions:

(i) The value of $|\nabla_h T|$ appropriate to the field of flow we have observed is much greater near the surface than the value suggested by climatological charts. Our estimated value of $|\nabla_h T|$ at the surface, 3·2° C/100 km, may, however, be a little high. At greater heights the value of $|\nabla_h T|$ decreases, and above 1 km it approaches the climatological value.

(ii) The measured value of the surface geostrophic wind component U_J $(Z=0)$ is somewhat overestimated. This implies that the values of τ_{YZ} in table 9, up to about 400 m at any rate, are somewhat overestimated. (The values of τ_{YZ} in table 8 are still larger overestimates.)

(iii) The revision of $\nabla_h T$ leaves the figures for τ_{XZ} and K_{XZ} in table 8 unaffected, since we have found no reason to make revisions of significant amount in either V_J $(Z=0)$ or $\partial V_J/\partial Z$. Moreover, the fair measure of agreement in the values of K_{XZ} in table 8 and of K_{YZ} in table 9 when the latter are adjusted in the direction implied by a lowering of U_J $(Z=0)$, encourages the belief that there is internal consistency in the revised findings.

TABLE 9. VALUES OF τ_{YZ} AND K_{YZ} FROM REVISED VALUES OF $U_J(Z)$ (CF. TABLE 8)

z (m)	τ_{YZ} (dyn/cm²)	K_{YZ} (10^5 cm²/s)
0	0	—
100	0·136	1·41
200	0·171	1·29
300	0·172	0·89
400	0·152	0·63
500	0·120	0·40
600	0·079	0·19
700	0·037	0·12
800	0·007	0·04
900	−0·007	—
1000	−0·017	—
1100	−0·018	—

Equality in the K's at 100 m could in fact be achieved by decreasing the surface geostrophic wind speed from the measured 10·1 m/s to 9·6 m/s and veering it $2\frac{1}{2}°$ on the measured direction. These changes could well represent the errors in our determination of **J**.* The revised value of **J** would then imply a change in the coefficient of surface drag c from $1{\cdot}24\times10^{-3}$ to $1{\cdot}50\times10^{-3}$.

8. PROPERTIES OF THE DAILY MEANS OF HORIZONTAL MOTION

The mean profiles of U and V for each day of observation are shown in figure 9 which also includes the direction of the surface wind, i.e. the direction of the X-axis to which U refers, and the number of ascents on which each pair of profiles is based. It is to be remembered that the data become somewhat inhomogeneous above about 750 m, and this is in

* The modification of **J** (veer $2\frac{1}{2}°$; reduction by 5 %) would imply that in the pressure-gradient triangle *JAC*, figure 3, the period-mean pressure at Anegada was 0·02 mb low, and that at St Croix 0·05 mb low, relative to San Juan. This error is quite possible.

Downloaded from rsta.royalsocietypublishing.org

evidence towards the top of a few of the curves, e.g. 14 March, where the scatter of points is greatest.

The profiles of U are all broadly of the form of the period-mean profile of U (figure 5). There is, however, a large variation in the height of the maximum, from 125 m on 19 March to 1150 m on 14 March and about 1400 m on 23 March,* and the turning point is very sharp on some days, e.g. 30 March, but broadly rounded on others, e.g. 24 March. A subsidiary maximum occurs on several days.

The profiles of V do not conform to a well-defined pattern. This component of the motion is commonly negative and increases numerically with height up to or beyond the level of maximum U, corresponding to an increasing veer of the wind with height, but the variation of V in the upper levels may be of either sense and may lead either to a further increase in veer with height or to a decrease. The profile of 3 April is notable for practically zero values of V up to the level of maximum U, i.e. a two-dimensional shearing-flow pattern up to this height, with increasing positive values of V above, so that the wind there *backs* with height —by 15° from 750 to 1350 m.

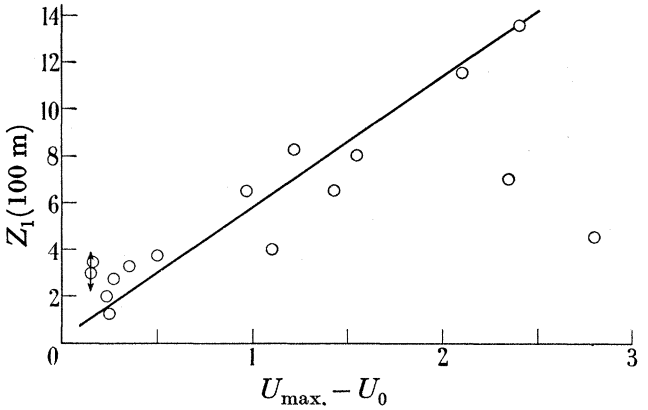

FIGURE 10. Variation of height, Z_1, of maximum value of U with difference of U between Z_1 and surface.

A profitable analysis of the daily profiles of U and V is hindered by lack of a realistic theory of the motion. We have, however, attempted to correlate the height Z_1 of the turning point of the U profile with other variables. The only success was with the velocity difference $(U_{max.} - U_0)$ shown in figure 10, which implies that the mean shear of the U component from the surface to the turning point is roughly constant. The physical significance of the relation is not apparent, nor, in view of the highly variable form of the profile, may it be very profitable to seek it.

There was no well-defined increase of Z_1 with U_0 as in Sheppard & Omar's (1952) analysis; this may be due to our taking daily mean values, whereas Sheppard & Omar used average values of 30 to 40 daily ascents in each of their wind groups.

The upper parts of the U profiles, well above the turning points, might be expected to provide a first approximation to the thermal wind in the direction of the X-axis, i.e. of the horizontal gradient of temperature in the direction of the Y-axis. Values of $\partial T/\partial Y$ implied by those profiles with a more or less clearly defined slope above the turning point are shown in table 10.

* Confirmed from radio wind observations at San Juan on 23 March.

Downloaded from rsta.royalsocietypublishing.org

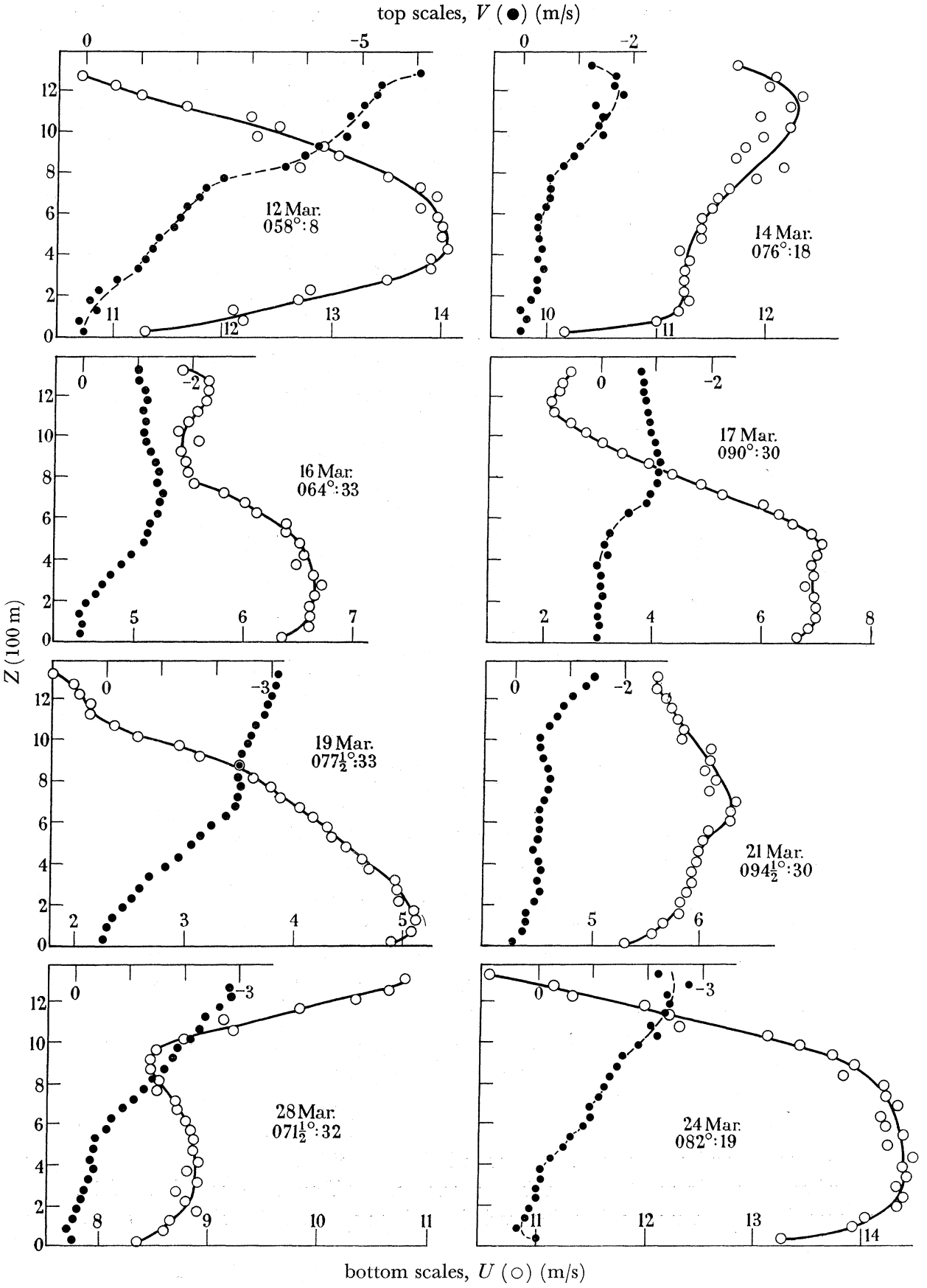

FIGURE 9. Daily mean profiles of wind components U (○) and V (●). The direction of the surface wind in degrees from true north, and the number of ascents upon which profiles are based, are shown under data. For other daily data see table 6.

PHILOSOPHICAL TRANSACTIONS OF THE ROYAL SOCIETY A MATHEMATICAL, PHYSICAL & ENGINEERING SCIENCES
PHILOSOPHICAL TRANSACTIONS OF THE ROYAL SOCIETY A MATHEMATICAL, PHYSICAL & ENGINEERING SCIENCES

Downloaded from rsta.royalsocietypublishing.org

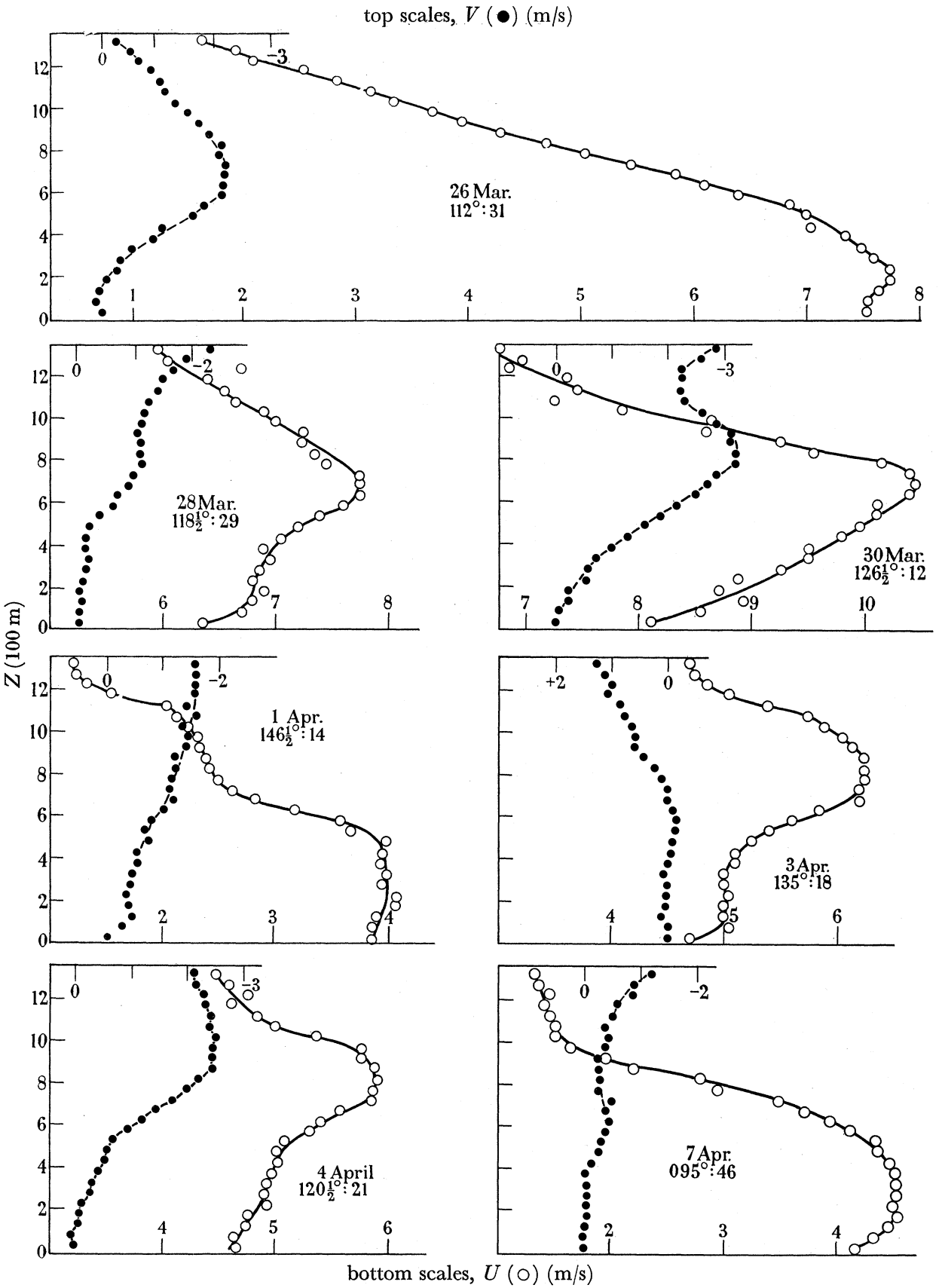

FIGURE 9 (*cont.*)

PHILOSOPHICAL TRANSACTIONS OF THE ROYAL SOCIETY A MATHEMATICAL, PHYSICAL & ENGINEERING SCIENCES
PHILOSOPHICAL TRANSACTIONS OF THE ROYAL SOCIETY A MATHEMATICAL, PHYSICAL & ENGINEERING SCIENCES

Downloaded from rsta.royalsocietypublishing.org

The values of $\partial T/\partial Y$ appear to be rather high, so that the slope of the upper part of the U-profile evidently exceeds in general that of the thermal wind unless the local value of the latter, even at heights greater than 500 m, is much greater than the climatological value for the surrounding area (cf. § 7·2). The result is of some interest, since the effect of vertical mixing by Trade cumuli and their associated motions is presumably to diminish the vertical gradient below that of the geostrophic wind. This suggests that larger-scale ageostrophic motions may exert a controlling influence in the opposite sense.

TABLE 10. SLOPES OF UPPER PARTS OF U-PROFILES AND CORRESPONDING HORIZONTAL TEMPERATURE GRADIENTS $\partial T/\partial Y$

date	$\partial U/\partial Z$ (m s^{-1}/100 m)	$\partial T/\partial Y$ (°C/100 km)	direction (deg.)
12 Mar.	0·59	0·81	148
19	0·36	0·50	167
21	0·14	0·19	185
24	0·74	1·02	172
26	0·67	0·92	202
28	0·31	0·42	209
30	0·57	0·79	217
1 Apr.	0·28	0·39	237
3	0·42	0·58	225
4	0·23	0·32	211
7	0·82 to 0·09	1·13 to 0·12	185

It is of interest to note from figure A 1 (Appendix) giving the plan trajectories of the balloons in groups of ascents on a daily or half-daily basis, that the veer of the wind with height is generally greatest when the surface wind is well south of east. This indicates that the variation of wind direction in the lowest kilometre or so of the Trades may be as much a reflexion of the thermal wind, which is predominantly zonal, as of frictional processes, a result also reached in our analysis of wind over the sea in the westerlies at the Scilly Isles (Sheppard *et al.* 1952).

A treatment of the momentum balance on a daily basis, in a manner similar to that used in § 7, has not proved possible because we could not determine with sufficient accuracy

(*a*) the accelerations $\mathrm{d}U/\mathrm{d}t$, $\mathrm{d}V/\mathrm{d}t$ which must now be included in the equations of momentum,

(*b*) the geostrophic wind and its variation with height.

We were, however, able to satisfy ourselves that, on a daily basis, some components of the acceleration were highly significant.

A much lengthier or more comprehensive series of observations would therefore be required to investigate, for example, the important question of the variation of drag coefficient c with surface wind velocity or the nature of the departures from the momentum balance expressed by equations (3) and (4).

9. PROPERTIES OF THE FLUCTUATIONS OF THE OBSERVED WIND

9·1. *Introduction*

The observations of wind made in Anegada were sufficiently detailed and accurate to provide data for an analysis of medium-scale turbulence in the field of flow (common in the Trades) where the mean surface wind and the thermal wind are opposed and where

Downloaded from rsta.royalsocietypublishing.org

cumulus convection is usually present. Fluctuations from the mean flow are therefore analyzed to provide some of the relevant statistics in relation to height and to the scale of motions studied. These statistics include estimates of intensity and of momentum transfer for motions on all scales observed.

9·2. *Observations*

The primary series of double-theodolite pilot-balloon ascents, which have been described in § 3, provided values of the three velocity components of the balloon at heights up to about 1350 m. Each component is a mean motion over the path followed by the balloon during a particular 20 s interval, which corresponds to about 50 m height. In earlier sections it was convenient to use co-ordinate axes fixed relative to the mean surface wind observed over a given period. In this section, for convenience, the axes used are fixed, the x-axis being horizontal and along the line from P to Q, 332° (see figure 1), the y-axis is horizontal and at right angles to the left and the z-axis vertical. The horizontal components of the wind u and v were obtained directly from the observations as was the vertical velocity of the balloon. The vertical velocity of the air can only be determined on the basis of assumptions which are detailed below.

9·3. *Determination of vertical component of air velocity*

The vertical component of air velocity over a 20 s interval, w, was obtained by subtracting from the observed vertical velocity of the balloon during that interval the mean velocity of the balloon throughout the particular ascent.

This assumes, first, that the vertical velocity of the balloon relative to the air does not vary with height and, secondly, that the mean vertical velocity of the air over any ascent is zero. Neither assumption can be completely verified with the data available, but there is some evidence to support the view that most of the indicated variation of w is due to air motion. Variations in the rate of ascent were not large (see table 3) and could well have been connected with small variations in shape (Ludlam 1953). The variations of the Reynolds number about its mean value were small, as were variations in the density in the layer from surface to 1350 m. Variations in the vertical velocity of the balloon relative to the air are likely to be small.

Table A 1 in the Appendix gives the mean vertical air velocities at various heights for selected groups of ascents. (Details of the height ranges used and of the composition of the groups selected are given later in table 12.) It will be seen that the mean vertical velocity is of order 10 cm/s, and that the pattern of its variation with height depends on the wind direction and is different for balloons released from the island and from the sea to windward of it. These results are not inconsistent with our first hypothesis that the vertical velocity of the balloon relative to the air does not vary with height; they imply that a particular distribution of mean vertical velocity is set up by the heated island. This pattern is further discussed in the Appendix; since it is in qualitative agreement with recent theoretical work on flow over heated islands (Malkus & Stern 1954; Smith 1955) it appears that the variation with height of the vertical velocity of the balloon relative to the air is probably considerably smaller than the indicated variation in vertical air velocity which is of order 30 cm/s.

PHILOSOPHICAL TRANSACTIONS OF THE ROYAL SOCIETY A MATHEMATICAL, PHYSICAL & ENGINEERING SCIENCES

PHILOSOPHICAL TRANSACTIONS OF THE ROYAL SOCIETY A MATHEMATICAL, PHYSICAL & ENGINEERING SCIENCES

Downloaded from rsta.royalsocietypublishing.org

9·4. *Statistics of fluctuations of wind*

The ascents of the primary series were divided into groups and the observations in each ascent divided into eleven ranges of time from release. For each group, and for the observations in each of eleven selected ranges of time from release shown in table 11, values of

$$\left.\begin{array}{lll} \bar{u}, & \bar{v}, & \bar{w}, \\ \overline{u'^2}, & \overline{v'^2}, & \overline{w'^2}, \\ \overline{u'v'}, & \overline{u'w'}, & \overline{v'w'}, \end{array}\right\} \qquad \text{(I)}$$

were calculated using the relations

$$\left.\begin{array}{l} n\bar{u} \equiv \sum_n u, \\ n\overline{u'^2} \equiv \sum_n u^2 - n\bar{u}^2, \\ n\overline{u'v'} \equiv \sum_n uv - n\bar{u}\bar{v}, \\ \text{etc.}, \end{array}\right\} \qquad \text{(II)}$$

where n is the number of observations in each range of time from release. In view of the small variations in the mean rate of rise of the balloon the time from release can be taken as equivalent to height, the selected mean heights being given in table 11.

TABLE 11. RANGES OF TIME FROM RELEASE USED TO GROUP OBSERVATIONS WITH RESPECT TO HEIGHT

height range	intervals from release over which velocities measured (s)	mean time from release (s)	approx. mean height (m)
a	0 to 20	10	25
b	20 to 40	30	75
c	40 to 60, 60 to 80, 80 to 100	70	175
d	100 to 120, 120 to 140, 140 to 160	130	325
e	160 to 180, 180 to 200, 200 to 220	190	475
f	220 to 240, 240 to 260, 260 to 280	250	625
g	280 to 300, 300 to 320, 320 to 340	310	775
h	340 to 360, 360 to 380, 380 to 400	370	925
i	400 to 420, 420 to 440, 440 to 460	430	1075
j	460 to 480, 480 to 500, 500 to 520	490	1225
k	520 to 540	530	1325

The largest group of ascents which could be used was clearly that containing all the ascents made. The smallest group which could reasonably be chosen contained ascents made during a particular day (say 7 h) or half-day (say 3 h). Groups selected on this basis are detailed in table 12. Selection was arbitrary but not, it is hoped, unreasonable; the choice makes it possible to determine the effect of releasing balloons from different points and at different times of day. Balloons in all these groups were tracked for at least 300 s from release (i.e. to about 750 m height) except for those in groups A and M which were followed to at least 240 s (600 m height) so that the data are homogeneous to these levels and usually beyond (cf. table 2).

Downloaded from rsta.royalsocietypublishing.org

TABLE 12. DETAILS OF GROUPS OF ASCENTS SELECTED FOR ANALYSIS

group	no. of ascents	release point	time of day	date 1953	balloons followed for minimum time of (s)	approx. minimum height reached (m)
A	13	*P*	a.m. and p.m.	12 Mar.	240	600
B	18	mainly *P*		14 Mar.		
C	17	*P*		16 Mar.		
D	16	*Q*		16 Mar.		
E	15	*P*, *Q* alternately	a.m.	17 Mar.		
F	15		p.m.	17 Mar.		
G	17	*P*	a.m. and p.m.	19 Mar.	300	750
H	16	*Q*		19 Mar.		
I	15	*P*, *Q* alternately	a.m.	21 Mar.		
J	15		p.m.	21 Mar.		
K	17	*P*	a.m. and p.m.	23 Mar.		
L	15	*Q*		23 Mar.		
M	13	*P*, *Q* alternately	a.m.	24 Mar.	240	600
N	13		p.m.	24 Mar.		
O	31	*P* and *Q*	a.m. and p.m.	26 Mar.		
P	29	mainly *P*		28 Mar.		
Q	12	*P*		30 Mar.		
R	14	boat		1 Apr.		
S	8	boat	a.m.	3 Apr.	300	750
T	10	boat	p.m.	3 Apr.		
U	10	boat		4 Apr.		
V	11	*Q*		4 Apr.		
W	23	*Q*	a.m.	7 Apr.		
X	24	*Q*	p.m.	7 Apr.		

9·5. *Effect of time of averaging*

The observed air motions are limited in scale, on the one hand by the instrumental technique of observation and on the other by the length of the period over which the observations were made. The scale of w is peculiarly limited by the technique used to determine this component of the motion. As described in § 9·3 we have only indirect information about vertical motions which are of greater time scale than the duration of an ascent.* It is difficult to specify precisely the small-scale, instrumental cut-off, but since each observed velocity is a mean over the (inclined) path of a balloon during a particular 20 s of its flight (i.e. over a layer some 50 m thick) the smallest motions observed have a 'period' greater than about 40 s and are at least 50 m in vertical extent. They are not affected by the motion of air round the balloon.

To investigate the effect of varying the time of averaging the observations have been separated into:

(i) The 24 groups A, B, ..., X detailed in table 12. Of these, six contain observations made during the whole of an observing day—say 7 h—and eighteen contain observations made during the morning or during the afternoon of an observing day—say 3 h.

(ii) Fifteen groups each containing observations made during one observing day, i.e. groups A, B, C and D, E and F, G and H, I and J, K and L, M and N, O, P, Q, R, S and T, U and V, W and X.

* But we intend also to extend our range of scale at a later date by using the suggestion made by Ludlam (1953) that the rate of rise of unloaded balloons such as ours is independent of their diameter and weight.

Downloaded from rsta.royalsocietypublishing.org

(iii) Five groups each containing observations made during 3 days of observation, i.e. groups A to D, E to J, K to O, P to R, S to X.

(iv) Three groups each containing observations made during 5 days of observation, i.e. groups A to H, I to P, Q to X.

(v) One group containing all the ascents of the primary series, i.e. 15 days of observation spread over 27 days in all.

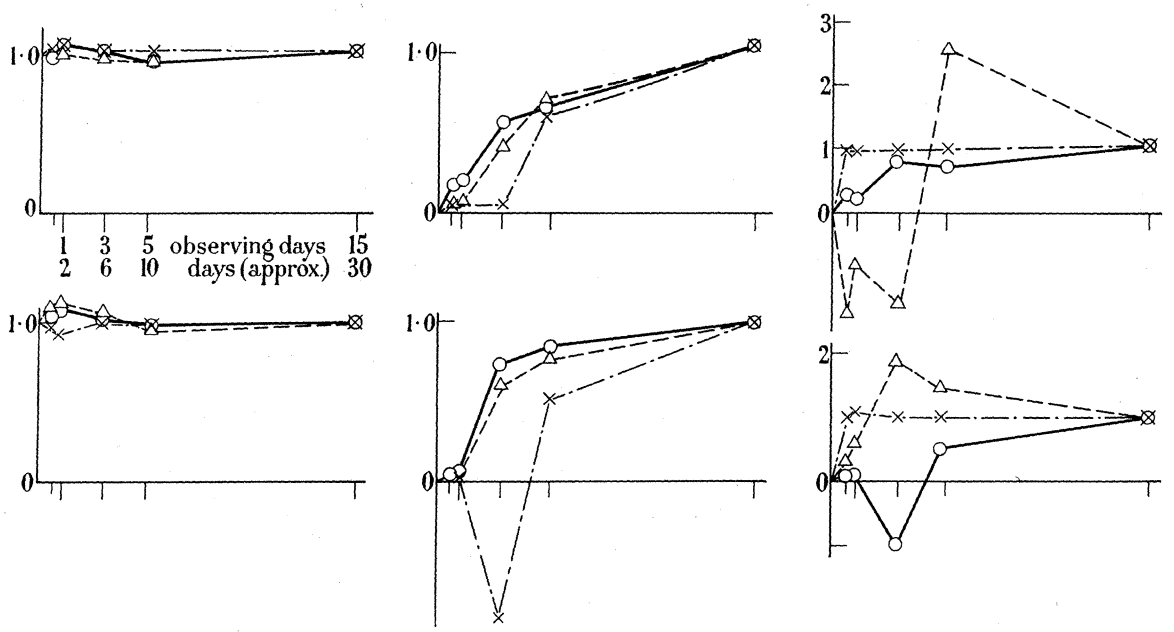

FIGURE 11. Variation with averaging period of wind fluctuation statistics from 15 days of observation for complete primary series. Total period of observation covered 27 days. The statistics are normalized by dividing by the value appropriate to the 15-day averaging period. Upper three graphs refer to height range (c), lower three to height range (g). Left-hand pair refer to mean motion $\bar{u}$ (○), $\bar{v}$ (△), $\bar{w}$ (×); middle pair to $\overline{u'^2}$ (○), $\overline{v'^2}$ (△), $\overline{u'v'}$ (×); right-hand pair to $\overline{u'w'}$ (○), $\overline{v'w'}$ (△), $\overline{w'^2}$ (×).

Data are available for all the height ranges of table 11, but to investigate the effect of changing the averaging period we have chosen to use the data for two particular height ranges, one above and one below the usual base of Trade cumuli. The height ranges selected are c (100 to 250 m) and g (700 to 850 m). The statistics have been evaluated for observations falling in these height ranges for ascents in all groups detailed in (i) to (v) above. The values computed from groups of a given averaging period, e.g. the three groups comprising (iv) above, are variable and the results, which are presented in figure 11, show the average values of the statistics for groups of a given averaging period.

The values of $\bar{u}$, $\bar{v}$ and $\bar{w}$ are, as may be expected, not affected significantly by the length of the averaging period. Their variation arises solely from the fact that groups of a given averaging period include differing numbers of ascents.

Computed values of $\overline{w'^2}$ are largely independent of the length of the averaging period. This is necessarily so since the technique used to determine w from the observations largely eliminates motions of time scale greater than the duration of an ascent. The result is, however, likely to be approximately valid for the whole range of scale of vertical motion in the

Downloaded from rsta.royalsocietypublishing.org

lowest kilometre. Computed values of $\overline{u'w'}$ and $\overline{v'w'}$ do not appear to vary systematically. Values of $\overline{u'^2}$, $\overline{v'^2}$ and $\overline{u'v'}$, however, in general increase as the averaging period increases.

The effect of the time of averaging on motions on a time scale less than that of the groups A, B, ..., X was investigated using ascents from groups W and X (7 April 1953). On this occasion forty ascents were made at 5 min intervals between 0930 and 1300. These forty ascents were subdivided into

(i) Eight groups each containing 5 consecutive ascents,
(ii) Four groups each containing 10 consecutive ascents,
(iii) Two groups each containing 20 consecutive ascents,
(iv) One group consisting of all 40 ascents in the series.

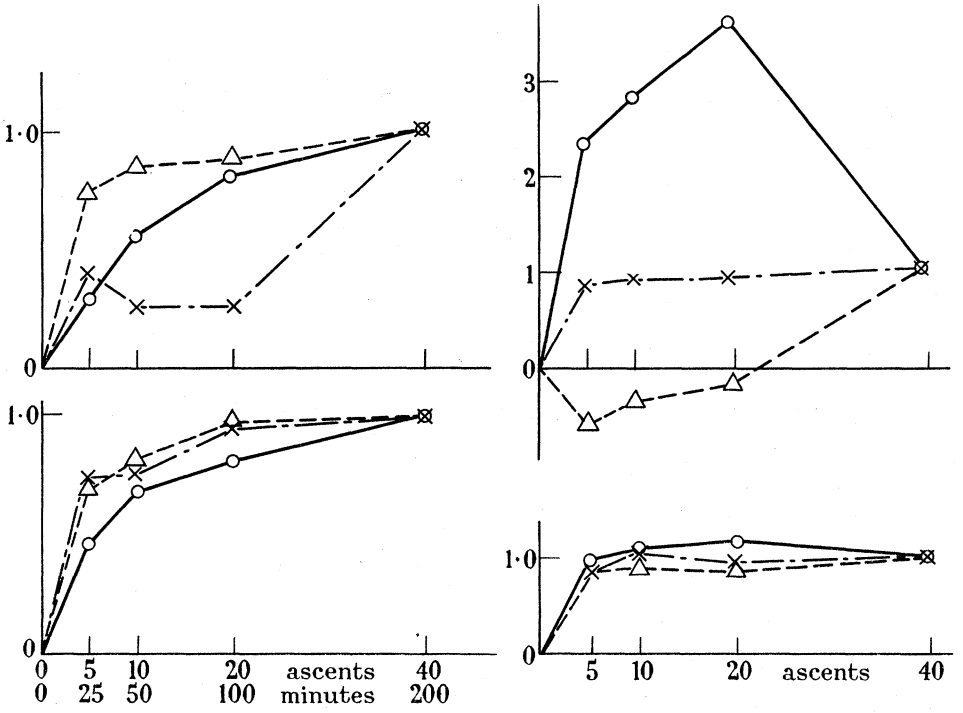

FIGURE 12. Variation with averaging period of wind fluctuation statistics from forty balloon ascents at 5 min intervals on 7 April 1953. The statistics are normalized by dividing by the value appropriate to all forty ascents. Upper pair of graphs refer to height range (*c*), lower pair to height range (*g*). Left-hand pair refer to $\overline{u'^2}$ (○), $\overline{v'^2}$ (△), $\overline{u'v'}$ (×); right-hand pair to $\overline{u'w'}$ (○), $\overline{v'w'}$ (△), $\overline{w'^2}$ (×).

The nine statistics (I) were computed for each group, again for the height intervals *c* (100 m to 250 m) and *g* (700 m to 850 m) of table 11. The results are again presented as average values for groups of a given length and are shown in figure 12.

In this case $\bar{u}$, $\bar{v}$ and $\bar{w}$ are constant by definition and the other statistics show similar behaviour to those computed from motions of longer time scale. $\overline{w'^2}$ remains independent of averaging period, although again this may be due to the technique for determining *w*. $\overline{u'w'}$ and $\overline{v'w'}$ again do not vary systematically. $\overline{u'^2}$, $\overline{v'^2}$ and $\overline{u'v'}$ again tend to increase with averaging period, providing evidence in this case of a trend in the values of *u* and *v*.

It is apparent that at these low levels in the Trades the transport of momentum in the

Downloaded from rsta.royalsocietypublishing.org

horizontal by motions of the scale observed is dominated by larger-scale components. The observed transport of momentum in the vertical is probably due to the smaller-scale components.

9·6. *Approximate lag covariances for large-scale horizontal motion*

The method used in § 9·5 was that of subdividing a series of observations of given duration into equal sections and then averaging the statistics obtained using each section separately. It has been used by earlier workers, such as Deacon (1955) and Swinbank (1955), as a crude form of spectral analysis. In this section some of the results of § 9·5 are used to deduce the likely form of the lag covariances appropriate to the large-scale horizontal motion we observed; if these are judiciously extrapolated they can be transformed by standard methods into the corresponding spectra.

The atmosphere contains motions of a wide range of time scale so that in general any statistics computed from observed data depend also on the averaging period used. The more obvious difficulties which arise have been discussed by Charnock & Robinson (1956) For our present purpose we imagine that we have available a long series of observations, extending over a time interval, say T, which is large compared with the 'period' of any component of the motion which contributes significantly to the total intensity or to the total transport. We define a normalized lag covariance, $R_{uv}(\tau)$, as an even function given by the equation

$$2R_{uv}(\tau)\int_0^T u(t)\,v(t)\,\mathrm{d}t \equiv \int_0^T u(t)\,v(t+\tau)\,\mathrm{d}t + \int_0^T u(t)\,v(t-\tau)\,\mathrm{d}t,$$

and similarly for $R_{uu}(\tau)$ and $R_{vv}(\tau)$. It should be noted that in this § 9·6 only, τ and T are time intervals such that $\tau \ll T$; they do not have the significance given in the list of symbols. We also define $F_{uu}(\tau)$, $F_{vv}(\tau)$ and $F_{uv}(\tau)$ by

$$[\overline{u'v'}]_T F_{uv}(\tau) \equiv [\overline{u'v'}]_\tau,$$

with two similar equations for $F_{uu}(\tau)$ and $F_{vv}(\tau)$. $[\overline{u'v'}]_\tau$ is here the average value of $\overline{u'v'}$ computed from series of observations each of duration $\tau \ll T$, and $[\overline{u'v'}]_T$ is the corresponding value appropriate to our hypothetical long series of observation. We shall refer to $[\overline{u'v'}]_T$ as the 'total' flux and $[\overline{u'^2}]_T$ and $[\overline{v'^2}]_T$ as 'total' intensities.

It can then be shown (see Charnock & Robinson 1956) that

$$\frac{1}{2}\frac{\mathrm{d}^2}{\mathrm{d}\tau^2}(\tau^2 F_{uv}(\tau)) = 1 - R_{uv}(\tau),$$

and $F_{uu}(\tau)$, $F_{vv}(\tau)$ are similarly related to $R_{uu}(\tau)$, $R_{vv}(\tau)$.

If we were to regard the data shown in figure 11 as providing reasonable curves of $F_{uv}(\tau)$, $F_{uu}(\tau)$ and $F_{vv}(\tau)$ we could compute corresponding values of $R_{uv}(\tau)$, $R_{uu}(\tau)$ and $R_{vv}(\tau)$. But the resulting values would clearly only be approximate since the data are very scattered and the relation above requires the curves of figure 11 to be normalized by dividing by the 'total' flux or 'total' intensity which of course we did not observe. In spite of these difficulties it seems useful to get even a crude picture of the form of the lag covariances for turbulence of this large and important scale which has not yet been much studied. We have accordingly approximated the data of figure 11 to give idealized curves shown in figure 13 for $F_{uu}(\tau)$, $F_{vv}(\tau)$ and $F_{uv}(\tau)$.

Downloaded from rsta.royalsocietypublishing.org

$F_{uu}(\tau)$ and $F_{vv}(\tau)$ are taken as the same, the 'total' intensity being chosen arbitrarily as 20 % greater than the intensity observed at $\tau = 15$ observing days. The corresponding curve for $R_{uu}(\tau)$ $(= R_{vv}(\tau))$ is shown in relation to τ in the upper right part of figure 13. In spite of the uncertainty the curve clearly shows the rapid decay of the lag covariance at small values of τ, $R_{uu}(\tau)$ becoming 0·5 at a value of τ of about 1 day. Similar values have been reported by Durst (1954) for winds observed by radar at 6 h intervals at all levels over Larkhill. The curve of $R_{uu}(\tau)$ against τ implies that motions of increasing period contain an increasing fraction of the 'total' energy.

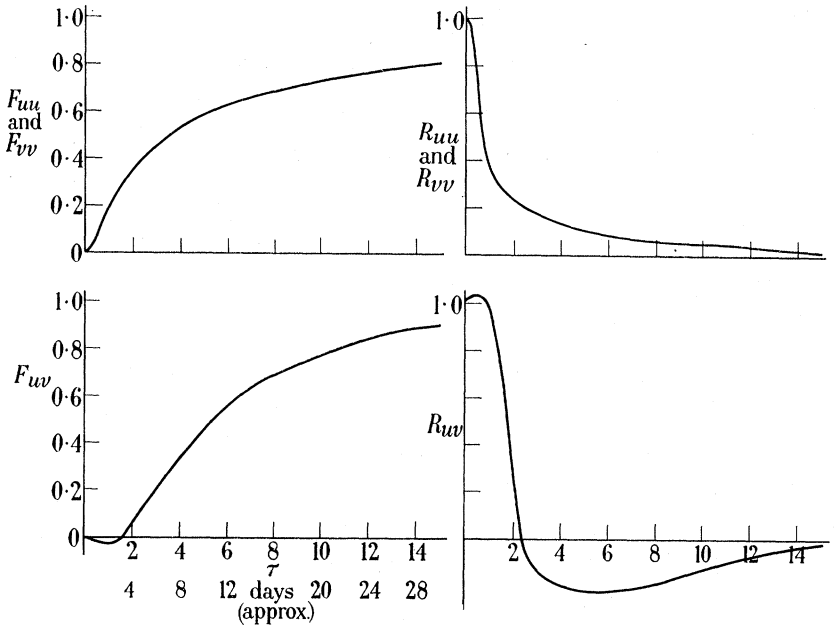

FIGURE 13. Idealized curves of F_{uu} or F_{vv} (above left), and F_{uv} (below left) in relation to averaging period, τ (observing days), based upon the experimental curves of figure 11; on their right-hand sides are the corresponding curves of R_{uu} or R_{vv} and R_{uv} also as functions of τ, derived from them (see text).

The values of $F_{uv}(\tau)$ shown in figure 11 are more scattered and their increase with τ is less clearly defined. At large values of τ, $F_{uv}(\tau)$ resembles $F_{uu}(\tau)$, but at small values there is an indication that $F_{uv}(\tau)$ becomes negative. This is confirmed by the results of later sections (9·7, 9·10), so that it is of interest to consider an assumed form for $F_{uv}(\tau)$ which shows this variation. Such an assumed form is shown in the lower left curve of figure 13. The value at $\tau = 1$ observing day is taken as negative and about $\frac{1}{30}$ of that at $\tau = 15$ observing days, our total period of observation. The latter value is taken as 0·9 time that of the 'total' flux. The corresponding variation of $R_{uv}(\tau)$ in the lower right-hand curve of figure 13 shows first an increase, at small values of τ, becoming greater than unity, then falling rapidly so that at larger values of τ it is predominantly negative and of decreasing magnitude.

We have chosen to define the lag covariance $R_{uv}(\tau)$ as an even function since we cannot by the present method determine the complete lag covariance, i.e. $r_{uv}(\tau)$, defined by

$$r_{uv}(\tau) \int_0^T u(t)\, v(t)\, \mathrm{d}t \equiv \int_0^T u(t)\, v(t+\tau)\, \mathrm{d}t,$$

PHILOSOPHICAL TRANSACTIONS OF THE ROYAL SOCIETY A MATHEMATICAL, PHYSICAL & ENGINEERING SCIENCES
PHILOSOPHICAL TRANSACTIONS OF THE ROYAL SOCIETY A MATHEMATICAL, PHYSICAL & ENGINEERING SCIENCES

Downloaded from rsta.royalsocietypublishing.org

but it seems likely that the initial rise of $R_{uv}(\tau)$ reflects a more marked asymmetry in the variation of $r_{uv}(\tau)$ from negative to positive values of τ. The implication is that a small amount of horizontal momentum is transferred by disturbances of small scale ('period' about 1 day), these disturbances being patterned in the sense that there is a higher correlation between the value of u at a given time and the value of v with a certain time delay than between simultaneous values of u and v. This point needs further investigation.

Values of $R_{uv}(\tau)$ for winds at 850 mb over the south-eastern United States have been presented by Estoque (1955). His curve exhibits rapid variation and does not behave like the one in figure 13 at small values of τ. Estoque obtains the spectrum of turbulent transfer

TABLE 13. AVERAGE VALUES OF STATISTICS OVER ALL GROUPS A, B, ..., X; FOR THE HEIGHT RANGES OF TABLE 11. UNITS ARE C.G.S.

Figures in italics are interpolated from smoothed curves.

height range table 11	mean height z (m)	mean motion $\bar{u}$ (cm/s)	mean motion $\bar{v}$ (cm/s)	mean motion $\bar{w}$ (cm/s)	variances $\overline{u'^2}$ (cm^2/s^2) $10\times$	variances $\overline{v'^2}$ (cm^2/s^2) $10\times$	variances $\overline{w'^2}$ (cm^2/s^2) $10\times$	$\left(\overline{u'^2}/\bar{u}^2\right)^{\frac{1}{2}}$ $10^{-2}\times$	$\left(\overline{v'^2}/\bar{v}^2\right)^{\frac{1}{2}}$ $10^{-2}\times$	$\overline{u'^2}/\overline{v'^2}$	$\overline{w'^2}/\overline{v'^2}$	gradients $\Delta u/\Delta z$ $10^{-4}\times$	gradients $\Delta v/\Delta z$ $10^{-4}\times$
a	25	288	527	14·5	962	693	82·0	34	16	1·39	0·118		
	50				*980*	*750*						19·0	45·0
b	75	298	549	17·0	985	758	111	33	16	1·30	0·146		
	125				*955*	*725*						17·0	7·7
c	175	315	557	9·5	913	665	114	30	15	1·37	0·171		
	250				*848*	*585*						14·7	− 1·3
d	325	337	555	0·3	815	530	69·5	27	13	1·54	0·131		
	400				*830*	*500*						17·7	−10·3
e	475	363	539	−4·5	883	505	60·0	26	13	1·75	0·119		
	550				*908*	*543*						20·3	18·7
f	625	394	511	−7·0	943	603	42·5	25	15	1·56	0·071		
	700				*1013*	*700*						9·3	−22·7
g	775	408	477	−5·5	1075	795	43·3	25	19	1·35	0·054		
	850				*1095*	*760*						− 3·0	−22·7
h	925	403	443	−3·5	1093	758	37·3	26	20	1·44	0·049		
	1000				*1075*	*755*						− 6·0	−18·7
i	1075	394	415	−1·5	1065	798	41·5	26	22	1·34	0·052		
	1150				*988*	*850*						−20·0	−26·3
j	1225	364	376	−1·0	915	958	46·5	26	26	0·956	0·049		
	1275				*888*	*975*						− 7·7	−17·0
k	1325	357	359	−0·1	868	993	54·0	26	28	0·874	0·054		

by a technique which minimizes the effect of the uncertainties: his result is broadly similar to the spectrum which would be obtained from our curve of $R_{uv}(\tau)$, indicating maximum transfer of horizontal momentum by motions of period several days. But our result cannot be given much significance, since the curve of $R_{uv}(\tau)$ is based on an assumed form for $F_{uv}(\tau)$ from observations made over a period of only 28 days. Observations over a much longer period would be required to provide more precise estimates.

9·7. *Intensity of smaller scale motions in relation to height*

To investigate the structure of the smaller-scale motions the statistics (I) were computed for each of the height ranges of table 11, the summations (II) being made over each of the groups specified in table 12 and also over groups of ascents made on a particular day, i.e. over the groups (i) and (ii) of § 9·5.

Section 8 has dealt with the variable form of the daily mean profiles of horizontal velocity and the values of the statistics computed on a daily and half-daily basis were also

Downloaded from rsta.royalsocietypublishing.org

found to be highly variable both with height and from group to group. In particular, the correlation coefficients r_{uv}, r_{uw}, r_{vw}, defined by

$$r_{uv} = \overline{u'v'}/(\overline{u'^2}.\overline{v'^2})^{\frac{1}{2}}, \quad \text{etc.},$$

were small (often less than 0·01) and inconsistent. They have no claim to significance, as was shown by computing the statistics (I) using fluctuations observed at different times, e.g. by using, say, u from one group with v from another. The resulting covariances and correlation coefficients were often of the same order as those appropriate to simultaneous fluctuations, so that the only argument for the significance of the statistics computed would lie in their smooth variation with height or with some other relevant variable. Since values of the covariances computed for these small groups of observations are of such doubtful significance they are not quoted here, but these data are available to anyone who wishes to make use of them.

		co-variances			correlation coefficients			eddy viscosities		statistics referred to axes X, Y		
$\frac{(\overline{u'^2})^{\frac{1}{2}}}{\Delta u/\Delta z}$ $10^4\times$	$\frac{(\overline{v'^2})^{\frac{1}{2}}}{\Delta v/\Delta z}$ $10^4\times$	$\overline{u'v'}$	$\overline{u'w'}$ (cm²/s²)	$\overline{v'w'}$	r_{uv}	r_{uw}	r_{vw}	$-\frac{\overline{u'w'}}{\Delta u/\Delta z}$ (cm²/s) $10^4\times$	$-\frac{\overline{v'w'}}{\Delta v/\Delta z}$ (cm²/s) $10^4\times$	$\overline{U'^2}$ $10\times$	$\overline{V'^2}$ (cm²/s²) $10\times$	$\overline{U'V'}$
		− 80·0	− 92·5	12·5	−0·010	−0·033	0·005			749	906	−1103
5·25	1·95	*− 425*	*−138*	*− 63*				7·2	1·4			
		− 700	−208	−105	−0·081	−0·063	−0·036			752	991	− 593
5·75	11·1	*− 900*	*−195*	*−135*				11·5	17·6			
		− 875	−198	−143	−0·112	−0·061	−0·052			649	929	− 585
6·30	−57·5	*−1625*	*−213*	*−140*				14·5	−105			
		−1875	− 15·0	−115	−0·285	−0·001	−0·060			438	907	− 215
5·10	− 6·90	*−2075*	*−188*	*− 60*				10·7	− 5·8			
		−2007	−158	213	−0·301	−0·068	0·122			424	964	− 537
4·65	− 3·90	*−1625*	*−113*	*37·5*				5·6	2·0			
		−1160	− 52·5	67·5	−0·154	−0·026	0·133			584	961	− 826
10·8	− 3·75	*− 750*	*− 42·5*	*77·5*				4·6	3·5			
		67·5	− 25·0	87·5	0·007	−0·012	0·047			867	1004	−1223
−34·9	− 3·90	*125*	*− 7·5*	*97·5*				−2·5	4·3			
		187·5	7·5	− 30·0	0·021	0·004	−0·018			852	998	−1519
−17·3	− 4·65	*925*	*82·5*	*115*				13·7	6·2			
		1220	168	133	0·132	0·080	0·073			964	899	−1782
− 4·95	− 3·45	*1450*	*250*	*188*				12·5	7·1			
		1628	320	268	0·174	0·155	0·127			1086	787	− 682
−12·3	− 5·80	*1750*	*350*	*350*				45·7	20·6			
		1805	370	455	0·195	0·171	0·197			1116	744	− 427

To get a gross picture of the structure of the observed fluctuations we have taken average values of the statistics at given heights, the average being taken over the twenty-four groups, A, B, ..., X. The resulting average values are given in table 13 and are shown in relation to height in figure 14. It will be seen that the correlation coefficients r_{uv}, r_{uw}, r_{vw} are still small, so that statistically the covariances have no *a priori* claim to significance. Nevertheless, these average values exhibit reasonably smooth variation with height and other relevant variables and are of considerable meteorological interest.

The mean velocities $\bar{u}$ and $\bar{v}$ are not precisely comparable, after a change of axes, with those of figure 5, because they are here the means of groups containing different numbers of ascents.

The average values of $\overline{u'^2}$ and $\overline{v'^2}$, and of $(\overline{u'^2}/\bar{u}^2)^{\frac{1}{2}}$ and $(\overline{v'^2}/\bar{v}^2)^{\frac{1}{2}}$, show little variation with height, although all show a tendency to decrease to a minimum at about 500 m and thereafter to increase. 500 m is near the average level of the base of the Trade cumuli. It must be borne in mind that balloons could only be followed in clear air so that statistics

Downloaded from rsta.royalsocietypublishing.org

computed from observations at higher levels are not necessarily typical of the whole flow field, although the effect of cloud on the horizontal velocities may well be small. The values of $(\overline{u'^2}/\bar{u}^2)^{\frac{1}{2}}$ range from 0·34 to 0·25 and values of $(\overline{v'^2}/\bar{v}^2)^{\frac{1}{2}}$ from 0·28 to 0·13. The difference in the two components cannot be immediately related to the mean motion because the orientation of our present axes is not chosen to relate to the wind, whose direction anyway varies with height. Values of $\overline{U'^2}$, $\overline{V'^2}$ and $\overline{U'V'}$ have been computed to give

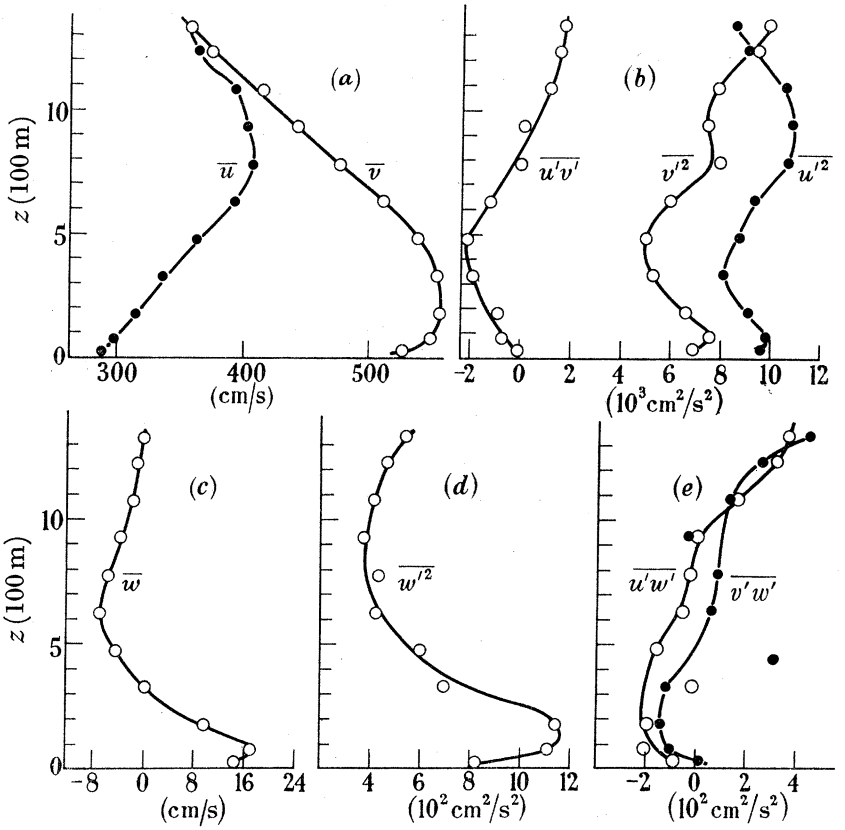

FIGURE 14. Variation with height of average values of wind fluctuation statistics from twenty-four groups specified in table 12.

statistics appropriate to axes orientated along and across the mean surface wind; these also are to be found in table 13. $\overline{U'^2}$ and $\overline{V'^2}$ are always of the same order, but $\overline{U'^2}$ decreases with height from the ground to reach a minimum at about 450 m and thereafter increases, showing a possible dependence on $\partial U/\partial z$; $\overline{V'^2}$ does not vary markedly with height. The sign of the product $\overline{U'V'}$ is consistently negative, i.e. it is such as to imply a transfer of westerly momentum by motions of this scale towards the south.

Values of $\overline{w'^2}$, after an initial rise in the lowest 200 m, decrease with height to a minimum near cloud base. The initial rise is no doubt a reflexion of the surface constraint on motions which at their smallest are of order 50 m deep. The later decrease is probably related to the increase of static stability with height. Values of $\overline{w'^2}$ appropriate to cloud would probably be much higher than those measured in clear air.

For motions on the range of scale analyzed there is no tendency to equipartition of turbulent energy between horizontal and vertical components. The ratio $\overline{u'^2}/\overline{v'^2}$ varies from

Downloaded from rsta.royalsocietypublishing.org

a maximum of 1·7 at 500 m to a minimum of 0·87 at 1325 m. The ratio $\overline{w'^2}/\overline{v'^2}$ varies from a maximum of 0·17 at 475 m to a minimum of 0·05 at 1325 m. The smallness of the latter ratio is probably due to the effect of the surface in suppressing the larger-scale components in w; the intensity of the horizontal motions is but little affected.

9·8. *Intensity of smaller-scale motions in relation to wind shear*

Table 13 also gives values of $(\overline{u'^2})^{\frac{1}{2}}(\Delta\bar{u}/\Delta z)^{-1}$ and $(\overline{v'^2})^{\frac{1}{2}}(\Delta\bar{v}/\Delta z)^{-1}$. To estimate the values for the wind shear $\Delta\bar{u}/\Delta z$ and $\Delta\bar{v}/\Delta z$, the values of $\bar{u}$ and $\bar{v}$ computed for the height ranges $a, b, \ldots, h$ of table 11 have been taken as appropriate to the mean height of observation in a given height range. $\Delta\bar{u}$ and $\Delta\bar{v}$ have then been calculated as differences between velocities at adjacent mean heights. Δz is taken as the difference in height between these adjacent mean heights, and the level midway between them is taken as the height to which the resulting values $\Delta\bar{u}/\Delta z$ and $\Delta\bar{v}/\Delta z$ refer. Values of $\overline{u'^2}$ and $\overline{v'^2}$ have then been read from the smooth curves of figure 14 at the height to which $\Delta\bar{u}/\Delta z$ and $\Delta\bar{v}/\Delta z$ refer.

The resulting values of $(\overline{u'^2})^{\frac{1}{2}}(\Delta\bar{u}/\Delta z)^{-1}$ and $(\overline{v'^2})^{\frac{1}{2}}(\Delta\bar{v}/\Delta z)^{-1}$ are scattered, but apart from extreme values, which occur with small values of $\Delta\bar{u}/\Delta z$ and $\Delta\bar{v}/\Delta z$, they are of order 500 m. These values provide a typical length for the turbulent flow analogous to Prandtl's mixing length. They are of the same order as the thickness of the layer in which the observations were made, and it is clear that the mixing length theory cannot be interpreted mechanistically for turbulence of large scale and high intensity which transports a relatively small amount of momentum. If such an interpretation be made, it appears that the product of 'typical length' and $(\overline{w'^2})^{\frac{1}{2}}$, neither of which vary markedly with height, is of order $10^6\,\mathrm{cm^2/s^{-1}}$, i.e. an order of magnitude greater than the values of K given in tables 8 and 9.

9·9. *Momentum transport as a function of height and wind shear*

Figure 14 also shows values of $\overline{u'w'}$ and $\overline{v'w'}$ as a function of height. These covariances are of special interest, since they are a measure of the vertical transfer of momentum by motions of the scale being analyzed. The total transfer of momentum due to motions on all scales observed has been estimated in an earlier section of this paper using observations of the vertical distribution of mean wind and of the pressure field. Tables 8 and 9 give the estimated components of shearing stress referred to axes along and across the mean surface wind. To compare these estimates with those made from our analysis of the fluctuations we have taken values of $\overline{u'w'}$ and $\overline{v'w'}$ from the smooth curves drawn by eye in figure 14. After multiplying by ρ (taken as $1{\cdot}2\times10^{-3}\,\mathrm{g/cm^3}$) and allowing for the rotation of the axes, the resulting values are directly comparable with those of τ_{XZ} and τ_{YZ} found in § 7. The comparison is shown in figure 15; the two sets of values are in fair agreement both in magnitude and in the form of their variation with height. The systematic differences in the layer 0 to 100 m are an indication that as the surface is approached the transport of momentum is brought about by motions on a progressively smaller scale. At these low levels our estimates of shearing stress from the fluctuation analysis are low because the observations do not include motions of sufficiently small scale. The chain-dotted line in figure 15 is a reasonable extrapolation from the values deduced from fluctuations above 100 m to the surface value of $0{\cdot}41\,\mathrm{dyn/cm^2}$ deduced in § 7.

PHILOSOPHICAL TRANSACTIONS OF THE ROYAL SOCIETY A MATHEMATICAL, PHYSICAL & ENGINEERING SCIENCES

PHILOSOPHICAL TRANSACTIONS OF THE ROYAL SOCIETY A MATHEMATICAL, PHYSICAL & ENGINEERING SCIENCES

Downloaded from rsta.royalsocietypublishing.org

That both sets of values agree at heights above 100 m is a notable result, indeed surprising in view of the small magnitude of the correlation coefficients r_{uw} and r_{vw} and of the difficulty in assessing the accuracy of our estimates, in particular the effect of our method of calculating values of w. The implication is that in the layer between 100 and 1350 m a large fraction of the total vertical transfer of momentum is brought about by the motions of 'period' between say 1 min and 4 h.

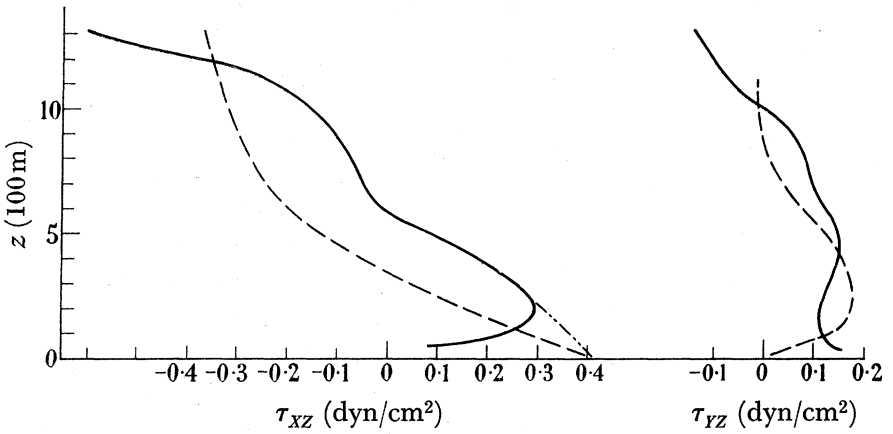

FIGURE 15. Comparison of shearing stresses estimated (*a*) by ageostrophic analysis of § 7 (dashed line), (*b*) by fluctuation analysis of § 9 (full line); chain-dotted line is an extrapolation (see text).

In view of the agreement shown in figure 15 we shall for the remainder of this § 9·9 refer to $-\rho\overline{u'w'}$ as τ_{xz} and $-\rho\overline{v'w'}$ as τ_{yz}. Values of $|\tau|/\rho \equiv (\tau_{xz}^2+\tau_{yz}^2)^{\frac{1}{2}}/\rho$ are shown in figure 16 in relation to height; again the dashed line is a reasonable extrapolation from the observed curve to the surface value of τ_0/ρ found independently in § 7. The minimum value occurs at about 750 m. Values of τ_{xz} and τ_{yz} have also been taken from the curves of figure 14 at heights which correspond to those used in the estimation of $\Delta\bar{u}/\Delta z$ and $\Delta\bar{v}/\Delta z$ as in § 9·8. It will also be seen from figure 16 that the direction of the vector formed by τ_{xz} and τ_{yz}, $\boldsymbol{\tau}$, is in moderate agreement with the direction of the vector formed by $\Delta\bar{u}/\Delta z$ and $\Delta\bar{v}/\Delta z$, that is $\Delta\mathbf{q}/\Delta z$, where the latter vector is well defined. This again is a notable, perhaps surprising, result.

In this § 9·9 we shall refer to

$$\frac{(\overline{u'w'}^2+\overline{v'w'}^2)^{\frac{1}{2}}}{((\Delta\bar{u}/\Delta z)^2+(\Delta\bar{v}/\Delta z)^2)^{\frac{1}{2}}}$$

as K, since it can be regarded as the contribution to the eddy viscosity from motions of the scale observed. Values of K in relation to height are shown in figure 16. They are reasonably consistent and of order 10^5 cm^2/s, as are the values of eddy viscosity deduced from the fields of mean wind and of mean pressure in § 7.

The relation of the flux to the gradient for the x and y co-ordinates separately, i.e. $-\overline{u'w'}(\Delta\bar{u}/\Delta z)^{-1}$ and $-\overline{v'w'}(\Delta\bar{v}/\Delta z)^{-1}$, are also listed in table 13. They are of the expected sense, the exceptions being near the maxima of $\bar{u}$ and $\bar{v}$ where the gradients are difficult to determine. The indicated values are of order 10^5 cm^2/s and do not differ systematically for flow in the two component directions.

Downloaded from rsta.royalsocietypublishing.org

The method used for estimating the shearing stress from the field of mean wind and of pressure described in §§2 and 7 is based on the assumption that the shearing stress $\tau_{xz}(\tau_{yz})$ vanishes where $\partial\bar{u}/\partial z(\partial\bar{v}/\partial z) = 0$. This assumption is to some extent supported by the above results of our analysis of the fluctuations.

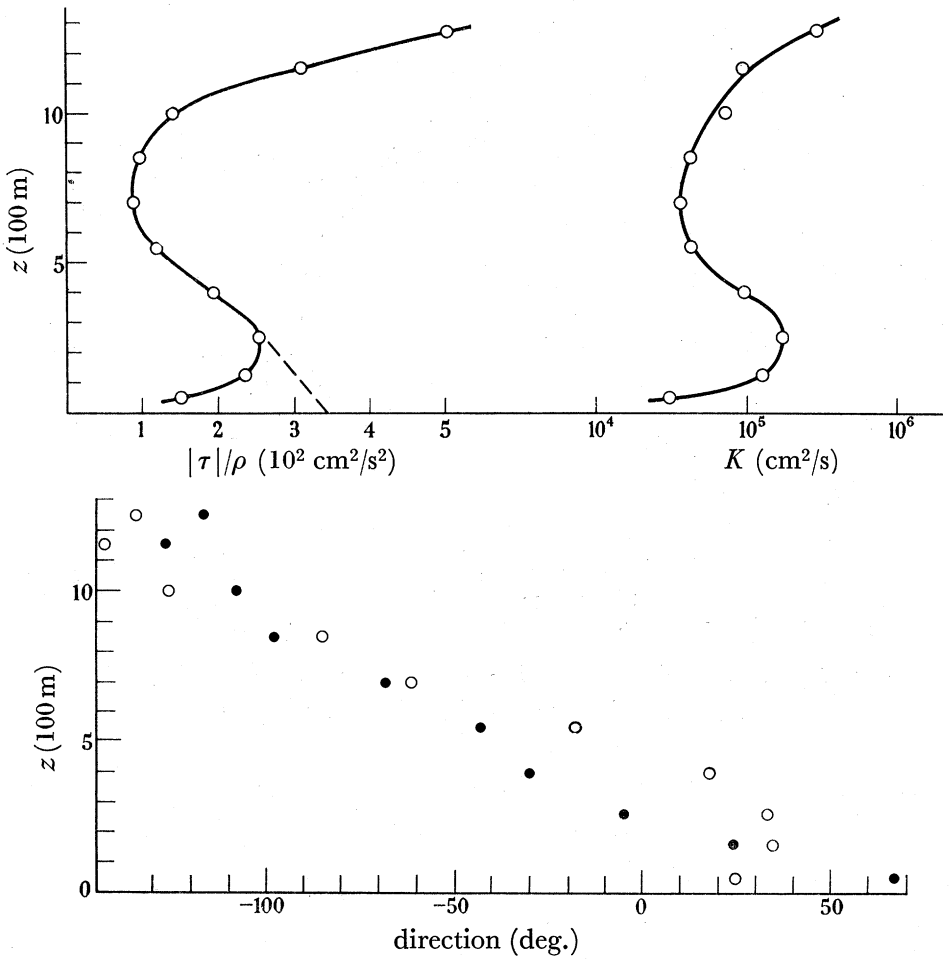

FIGURE 16. (Top) Variation with height of $|\tau|/\rho$ and of eddy viscosity, K, as found from fluctuation analysis. The dashed line is an extrapolation of $|\tau|/\rho$ (see text). (Bottom) Comparison of directions of shearing stress vector, $\boldsymbol{\tau}$(○), from fluctuation analysis, and of mean shear vector, $\Delta\mathbf{q}/\Delta z$ (●). Directions are in degrees from the x axis.

The values of $\overline{u'v'}$ shown plotted against height in figure 14 call for little comment other than that of § 9·7, although the change of sense at about 800 m may be worth noting. It is clear that motions on this scale are responsible for only a small part of the total transfer of momentum in the horizontal. A similar result is also implied in the analysis by Priestley (1949) for winds at all levels over Larkhill.

9·10. *Statistics computed from larger-scale motions*

Values of the nine statistics (I) have been computed using all the ascents of the primary series together. The resulting statistics are typical of motions on all scales from about a minute up to several days. The results are shown in table 14 and figure 17.

Downloaded from rsta.royalsocietypublishing.org

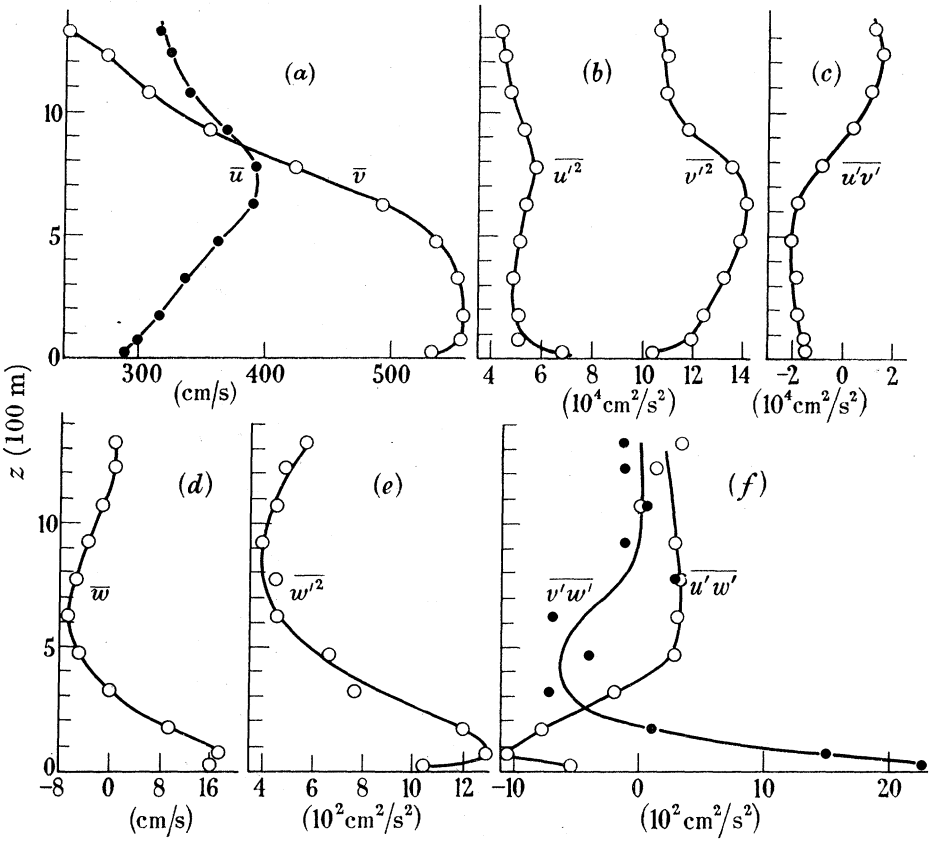

FIGURE 17. Variation with height of wind fluctuation statistics from all ascents of primary series taken as one group.

TABLE 14. STATISTICS FOR ALL ASCENTS OF THE PRIMARY SERIES TAKEN AS A SINGLE GROUP. UNITS ARE C.G.S.

Figures in italics are interpolated from smoothed curves.

height range table 11	mean height z (m)	mean motion $\overline{u}$	$\overline{v}$ (cm/s)	$\overline{w}$	variances $\overline{u'^2}$ $10^2\times$	$\overline{v'^2}$ (cm^2/s^2) $10^2\times$	$\overline{w'^2}$ $10^2\times$	$\left(\frac{\overline{u'^2}}{\overline{u}^2}\right)^{\frac{1}{2}}$ $10^{-2}\times$	$\left(\frac{\overline{v'^2}}{\overline{v}^2}\right)^{\frac{1}{2}}$ $10^{-2}\times$	$\frac{\overline{u'^2}}{\overline{v'^2}}$	$\frac{\overline{w'^2}}{\overline{v'^2}}$	gradients $\frac{\Delta u}{\Delta z}$ $10^{-4}\times$	$\frac{\Delta v}{\Delta z}$ $10^{-4}\times$
a	25	290	533	15·8	683	1040	10·4	90	65	0·657	0·010		
	50				*588*	*1135*						19·0	44·0
b	75	299	555	17·2	507	1199	12·9	75	63	0·423	0·011		
	125				*505*	*1220*						17·0	2·5
c	175	316	558	9·1	509	1247	12·0	71	63	0·409	0·010		
	250				*480*	*1288*						13·7	− 3·3
d	325	337	553	−0·1	490	1326	7·7	66	66	0·369	0·006		
	400				*503*	*1363*						17·0	−11·7
e	475	362	535	−5·2	514	1392	6·6	63	70	0·369	0·005		
	550				*525*	*1413*						18·3	−29·0
f	625	390	492	−6·8	539	1413	4·5	60	76	0·381	0·003		
	700				*556*	*1395*						2·0	−46·0
g	775	393	423	−5·7	570	1357	4·5	61	87	0·420	0·003		
	850				*558*	*1273*						−16·0	−45·0
h	925	369	355	−3·9	529	1180	3·9	62	97	0·448	0·003		
	1000				*500*	*1133*						−19·3	−32·7
i	1075	340	306	−1·7	474	1095	4·4	64	108	0·433	0·004		
	1150				*460*	*1093*						−10·0	−21·3
j	1225	325	274	0·2	454	1098	4·9	66	121	0·413	0·004		
	1275				*445*	*1081*						− 8·0	−30·7
k	1325	317	243	0·2	439	1073	5·7	66	135	0·409	0·005		

Downloaded from rsta.royalsocietypublishing.org

The distribution of mean horizontal velocity is necessarily similar to that computed from the smaller-scale motions. The values of $\overline{u'^2}$ and $\overline{v'^2}$ on this broad range of scale are much larger than those of the smaller scale. They show little variation with height; values of $(\overline{u'^2}/\overline{u}^2)^{\frac{1}{2}}$ range from 0·6 to 0·9 and values of $(\overline{v'^2}/\overline{v}^2)^{\frac{1}{2}}$ from 0·6 to 1·3. Values of $\overline{U'^2}$ and $\overline{V'^2}$ have again been computed to give statistics appropriate to axes along and across the mean surface wind. They are given in table 14 and show little variation with height.

Values of $\overline{u'v'}$ are shown in relation to height in figure 17; they are also listed in table 14 together with values of $\overline{U'V'}$, the corresponding statistic for axes along and across the mean surface wind direction 091°. The values of $\overline{U'V'}$ are consistently positive, indicating a transfer of westerly momentum toward the north at all levels. They are computed from a small sample but may suffice to show the order of magnitude of this transfer in the lowest kilometre of the Trades. The values are greater by a factor of about ten and of different sign than those computed from motions of smaller scale. Although we have no reason to believe that motions of larger scale would not yield even larger values of $\overline{U'V'}$ it is encouraging to note that the present values agree in sign and are comparable in magnitude with those derived by Starr & White (1952, 1954) from a much more extensive analysis of synoptic data.

It has already been pointed out that the technique adopted to determine w restricts $\overline{w'^2}$ to small-scale components of the flow. The close similarity in the values of $\overline{w'^2}$ in tables 13 and 14 is evidence of this.

The computed values of the statistics indicate that on the larger scales now included there is even less tendency to equipartition of turbulent energy in the horizontal and vertical directions. The ratio $\overline{u'^2}/\overline{v'^2}$ is of order 0·4 and the ratio $\overline{w'^2}/\overline{v'^2}$ is usually less than 0·01.

Table 14 also gives values of $(\overline{u'^2})^{\frac{1}{2}}(\Delta\bar{u}/\Delta z)^{-1}$ and $(\overline{v'^2})^{\frac{1}{2}}(\Delta\bar{v}/\Delta z)^{-1}$. The values of $\Delta\bar{u}/\Delta z$ and $\Delta\bar{v}/\Delta z$ have been calculated as before, and again the values of $\overline{u'^2}$ and $\overline{v'^2}$ have been read

		co-variances			correlation coefficients			eddy viscosities		statistics referred to axes X, Y		
$\frac{(\overline{u'^2})^{\frac{1}{2}}}{\Delta u/\Delta z}$	$\frac{(\overline{v'^2})^{\frac{1}{2}}}{\Delta v/\Delta z}$	$\overline{u'v'}$	$\overline{u'w'}$ (cm²/s²)	$\overline{v'w'}$				$-\frac{\overline{u'w'}}{\Delta u/\Delta z}$ (cm²/s)	$-\frac{\overline{v'w'}}{\Delta v/\Delta z}$	$\overline{U'^2}$	$\overline{V'^2}$ (cm²/s²)	$\overline{U'V'}$
$10^4\times$	$10^4\times$	$10\times$	$10\times$	$10\times$	r_{uv}	r_{uw}	r_{vw}	$10^4\times$	$10^4\times$	$10^2\times$	$10^2\times$	$10^2\times$
		−1493	− 55	228	−0·177	−0·065	−0·219			829	894	230
12·8	7·7	*−1513*	*− 88*	*178*				46·1	− 40·5			
		−1530	−105	150	−0·196	−0·130	0·121			906	799	375
13·2	139·7	*−1638*	*− 88*	*55*				51·5	−219			
		−1800	− 78	10	−0·226	−0·099	0·008			921	835	408
16·1	−107·7	*−1863*	*− 50*	*−40*				36·6	−120			
		−1875	− 20	−73	−0·233	−0·033	−0·072			970	845	454
13·2	− 31·7	*−2025*	*5*	*−63*				− 2·9	− 53·6			
		−2045	28	−40	−0·242	0·047	−0·042			1012	893	481
12·5	− 12·9	*−2000*	*30*	*−58*				− 16·4	− 19·8			
		−1820	30	−70	−0·209	0·061	−0·088			1053	899	467
117·9	− 8·1	*−1450*	*33*	*−30*				−163	− 6·5			
		− 850	33	30	−0·097	0·064	0·038			1100	827	379
−14·7	− 8·0	*− 225*	*30*	*− 5*				18·8	− 1·1			
		423	28	−13	0·054	0·060	−0·018			1063	646	254
−11·6	− 10·4	*775*	*28*	*0*				14·3	0			
		1148	0	5	0·159	0	0·007			1047	523	203
−21·5	− 15·5	*1350*	*23*	*0*				22·5	0			
		1610	13	−13	0·228	0·027	−0·017			1083	468	188
−26·4	− 10·7	*1550*	*20*	*0*				25·0	0			
		1298	33	−13	0·189	0·065	−0·016			1034	478	204

Downloaded from rsta.royalsocietypublishing.org

off the smooth curves of figure 17 at appropriate heights. Values of both $(\overline{u'^2})^{\frac{1}{2}}(\Delta\bar{u}/\Delta z)^{-1}$ and $(\overline{v'^2})^{\frac{1}{2}}(\Delta\bar{v}/\Delta z)$ are of order 1 km, except for some higher values which occur near the maxima of $\bar{u}$ and $\bar{v}$ where the gradients are difficult to determine.

Figure 17 also shows values of $\overline{u'w'}$ and $\overline{v'w'}$ as a function of height. The indicated transfer of momentum does not agree with the estimates of § 7. The correlation coefficients r_{uw} and r_{vw} are even smaller than for motions of smaller scale, and the present estimates are thought to be much the less reliable. This may be due to the inadequacy of our technique for determining w, but it is more likely to be due to our necessarily inadequate sampling of larger-scale motions which do not, on average, contribute to the total transfer of momentum.

9·11. *A critical perspective of fluctuation analysis*

Any investigation of atmospheric turbulence depends on the site and the exposure, accuracy and response of the instruments, as well as on the duration of the observations and on the technique and accuracy with which they are analyzed.

The present observations were designed to determine the turbulent structure of oceanic Trade-wind air. Although the site was the best we could find it is possible that some of our results were influenced by the presence of the island, small and flat though it was. The pilot-balloon technique was adequate in speed and accuracy for investigating turbulence on the range of scale which has so far received little attention. Its more serious limitations were that balloons were necessarily only observed in clear air (horizontal velocities can be expected to be typical of the whole field of flow but vertical velocities may not have been) and, more seriously, that the technique used to eliminate the vertical velocity of the balloons also eliminated vertical air velocities of large scale. The effect of this latter limitation is almost impossible to assess.

The correlation coefficients which result are small; they have no *a priori* claim to significance. This is a necessary result for motions of large scale and intensity whose momentum transport is of the order of the drag of the wind on the sea. Nevertheless, the statistics behave systematically with height and with other variables and some agree tolerably with estimates made independently.

In spite of these limitations we believe that the statistics provide useful information; a large amount of observational and analytical work remains before we have an adequate description of the turbulent structure of Trade-wind air.

Acknowledgements

It is pleasing to recall how little formality was required in the organization of the meteorological measurements described, although they involved an oversea expedition and the help of many people of different nations.

We are grateful for financial assistance from the Royal Society, the Governors of Imperial College, and from the National Oceanographic Council. We received much help and information from the Colonial Office, London, and from the Colonial Government of the Leeward Islands. The Directors of the Meteorological Office, London, and of the Weather Bureau, Washington, lent us apparatus and made specially available many data concerning the weather in the period during which we worked. The Director of the British Caribbean

PHILOSOPHICAL TRANSACTIONS OF THE ROYAL SOCIETY A MATHEMATICAL, PHYSICAL & ENGINEERING SCIENCES

PHILOSOPHICAL TRANSACTIONS OF THE ROYAL SOCIETY A MATHEMATICAL, PHYSICAL & ENGINEERING SCIENCES

Downloaded from rsta.royalsocietypublishing.org

Meteorological Service arranged for special observations of pressure and temperature to be taken and sent to us from a number of stations in the Leeward Islands. We are also indebted to the Hydrographer of the Navy, who arranged naval transport for the return of our equipment and to the Director of the National Physical Laboratory who provided the facilities of the Hollerith section for much of our computation.

It is a particular pleasure to record the great assistance rendered to us by Mr J. M. Monsanto, of St Thomas, who acted as our agent and kept open our lines of communication with his light aircraft. Similarly, our friends living on the island helped us in many ways.

Dr G. B. Tucker and Mr S. Williams accompanied us on the expedition, and their keenness and skill in taking observations and attending to other needs have contributed in no small manner to such success as the expedition has achieved. Mrs P. Edwards, of the National Institute of Oceanography, has made many of the subsequent calculations with patience and accuracy. Mrs D. Martin, of Imperial College, has prepared the manuscript for the printer.

There remains to mention our colleagues from the Woods Hole Oceanographic Institution who made related observations from the air in our vicinity; they helped us in many ways. Their work will be reported separately.

Appendix. The effect of a small island on the oceanic Trades

A 1. *Introduction*

We have already remarked in § 5 on the effect of the island and neighbouring shallow water in producing a characteristic pattern of convective cloud a few hours on either side of noon. This and any other disturbance of the general flow field by the island is of interest on its own account and especially in relation to our attempt to obtain representative values for many of the properties of the oceanic Trades for the area and time of year.

The data for ascents from different release points of balloons (stations P, Q and B, figure 1) in the primary series, and from some simultaneous ascents from stations Q and J on opposite sides of the island give material on which some assessment of the local disturbance may be made.

A 2. *The field of mean vertical motion produced by the island*

Assume, as in § 9, that the velocity of the balloon relative to the air is constant during each sounding and that the mean vertical motion of the air over a complete sounding is zero. The vertical velocity of the air, w, during a particular 20 s (50 m) interval of a balloon's flight is then the height increment measured during that 20 s less the average height increment for that particular flight. For a group of soundings, the mean vertical velocity $\overline{w}$ at a given height is then obtained by averaging the vertical velocities for that height in the group. The values of $\overline{w}$ so obtained for the groups of ascents used in § 9 are listed in table A 1, some smoothing being applied by averaging $\overline{w}$ over groups of three consecutive 20 s intervals after the first two intervals, which are both of 20 s, and up to the penultimate interval. (See left-hand columns of table A 1, wherein height increases upward from the *bottom* of the table.) The first two intervals are given separately because the variation of $\overline{w}$ with height z is likely to be most pronounced near the surface. Table A 1 is separated into three parts according to the wind direction, so that the variation of $\overline{w}$ may be examined more readily for dependence on the relevant variables.

Downloaded from rsta.royalsocietypublishing.org

TABLE A1. MEAN VERTICAL VELOCITY $\overline{w}$ (CM/S) AS A FUNCTION OF HEIGHT FOR ALL GROUPS OF ASCENTS

Mean vertical velocity of air over each ascent assumed zero. Ascending air in bold type; descending air in ordinary type.

(*a*) Mean trajectory direction 069 to 088°

group	A	B	M	N	K	L	C	D
time of day	all	all	a.m.	p.m.	all	all	all	all
U_0 (m/s)	11·29	10·13	13·05	13·2	8·36	8·32	6·32	6·40
θ_0 (deg.)	057½	075	081½	080½	071	073	065	063½
release from height (m)	*P*	*P* mainly	*P*, *Q*	*P*, *Q*	*P*	*Q*	*P*	*Q*
1275	−28	− 5	—	**+15**	− 2	−10	**+ 6**	− 4
1225	−30	− 1	—	**+ 9**	**+ 3**	− 4	**+ 0·5**	− 2
1075	− 9	**+ 0·5**	—	**+ 6**	**+11**	−10	− 8	− 4
925	−14	**+ 5**	**+ 9**	− 5	**+ 3**	−14	− 8	− 8
775	− 5	**+ 2**	− 2	− 6	− 8	−17	− 9	− 8
625	−24	−13	− 3	−17	−10	− 7	−10	− 4
475	−19	−16	− 5	− 9	−11	**+ 4**	− 5	**+ 4**
325	− 1	−12	− 8	− 4	− 8	**+10**	**+ 9**	**+ 9**
175	**+26**	**+ 5**	**+ 0·5**	**+11**	**+11**	**+20**	**+15**	**+ 7**
75	**+41**	**+38**	**+18**	**+20**	**+22**	**+20**	**+24**	**+ 7**
25	**+43**	**+34**	**+23**	**+34**	**+ 8**	**+12**	**+17**	**+11**
$\overline{W}$ (m/20 s)	51·6	48·7	51·9	49·0	50·6	52·0	50·3	51·3
departure of $\overline{W}$ from 49·5 m/20 s	+ 2·1	− 0·8	+ 2·4	− 0·5	+ 1·1	+ 2·5	+ 0·8	+ 1·8

(*b*) Mean trajectory direction 090 to 111°

group	I	J	G	H	X	W	E	F
time of day	a.m.	p.m.	all	all	p.m.	a.m.	a.m.	p.m.
U_0 (m/s)	5·63	4·97	5·00	4·74	4·65	4·65	3·42	3·29
θ_0 (deg.)	098	091	079½	075½	101½	088½	096½	083½
release from height (m)	*P*, *Q*	*P*, *Q*	*P*	*Q*	*Q*	*Q*	*P*, *Q*	*P*, *Q*
1275	**+ 3**	− 7	− 4	− 7	**+ 8**	**+12**	**+ 7**	− 7
1225	**+ 2**	−10	− 3	− 3	**+ 8**	**+ 6**	**+ 4**	− 4
1075	− 5	− 8	**+ 0·5**	− 2	**+ 2**	**+ 5**	**+ 6**	− 4
925	− 3	− 8	**+ 3**	− 8	− 8	**+ 3**	− 2	−12
775	− 1	− 3	− 2	− 9	− 8	− 2	−13	−10
625	**+ 0·5**	**+ 1**	**+ 3**	− 6	− 6	− 9	−13	− 8
475	**+ 2**	**+ 3**	− 3	− 4	−18	− 9	− 0·5	−13
325	− 6	**+ 8**	− 5	**+ 5**	− 7	− 3	**+ 5**	**+ 7**
175	**+ 3**	**+ 8**	− 2	**+14**	**+21**	**+ 0·5**	− 0·5	**+28**
75	**+ 6**	**+ 7**	**+14**	**+19**	**+25**	**+15**	**+10**	**+33**
25	**+15**	**+26**	**+ 5**	**+19**	**+20**	**+17**	**+12**	**+20**
$\overline{W}$ (m/20 s)	50·0	50·7	50·3	49·4	47·8	49·3	49·5	50·8
departure of W from 49·5 m/20 s	+ 0·5	+ 1·2	+ 0·8	− 0·1	− 1·7	− 0·2	0	+ 1·3

(*c*) Mean trajectory direction 124 to 136°

(*d*) mean traj. dirn 165°

group	Q	P	S	O	V	U	T	R
time of day	a.m.	all	a.m.	all	all	all	p.m.	all
U_0 (m/s)	8·10	6·37	5·36	7·50	4·73	4·60	4·10	3·86
θ_0 (deg.)	125	118½	139	112½	120½	121	130½	146½
release from height (m)	*P*	*P*, *Q*	*B*	*P*, *Q*	*Q*	*B*	*B*	*B*
1275	**+ 5**	− 2	**+17**	− 3	**+ 7**	− 5	− 2	− 3
1225	− 5	− 3	—	**+ 3**	**+ 4**	− 2	− 2	0
1075	−13	− 2	− 3	− 3	**+ 3**	**+ 2**	− 0·5	− 4
925	− 6	− 3	− 4	− 2	**+11**	**+ 1**	− 6	− 8
775	− 6	− 4	− 7	− 7	**+ 1**	− 2	− 3	−10
625	− 4	− 2	− 9	− 6	−16	**+ 1**	− 2	−13
475	**+ 3**	− 0·5	− 3	− 5	−15	**+ 4**	**+ 6**	− 5
325	**+10**	**+ 2**	− 3	− 4	−20	**+ 4**	**+ 4**	**+14**
175	**+11**	**+ 3**	**+20**	**+ 3**	**+ 4**	**+ 7**	**+ 4**	**+17**
75	**+ 6**	**+ 7**	**+22**	**+20**	**+19**	−11	**+15**	**+12**
25	**+ 2**	**+ 8**	**+ 5**	**+27**	**+30**	−18	− 6	− 7
$\overline{W}$ (m/20 s)	48·7	48·6	47·3	49·5	46·3	46·1	46·5	49·1
departure of $\overline{W}$ from 49·5 m/20 s	− 0·8	− 0·9	− 2·2	0	− 3·2	− 3·4	− 3·0	− 0·4

Downloaded from rsta.royalsocietypublishing.org

The values of $\overline{w}$ are necessarily small, and it is therefore appropriate to consider their possible error in the light of errors of observation and the assumptions on which they are based. Since the standard error in the measurement of vertical displacement has been shown (§ 3·3) to be about 1 m, the standard error in $\overline{w}$ for a 20 s interval in groups of 10 to 30 ascents is about 0·2 m/20 s or 1 cm/s, and rather less than this for means of three consecutive intervals. These errors are acceptable in the light of the values of $\overline{w}$ which lie mainly in the range ± 20 cm/s. Again, if the velocity of the balloon relative to the air varies systematically with height, a spurious variation in $\overline{w}(z)$ of like form would appear. But such variation if present would probably be monotonic whereas the actual variation of $\overline{w}(z)$ in most cases is not, e.g. $\overline{w}$ may be positive at lower levels, then negative and finally positive. The pattern of $\overline{w}(z)$ also changes from group to group, whereas any variation with height in the motion of the balloon relative to the air would probably be of the same form in all groups. We conclude therefore that such variation, if present, is too small to obscure the pattern of the vertical motion of the air though slight distortion is not be excluded. Since all ascents of the primary series were made with the sun well above the horizon, when a pattern of mean vertical motion of the air was probably more or less well developed, it is hardly profitable to attempt any further investigation of the adequacy of the assumption concerned.

The further assumption that the mean vertical motion of the air over a complete sounding is zero is less likely to be satisfied and is, moreover, also susceptible of some test. Thus the mean rate of balloon ascent $\overline{W}$ over complete (not necessarily full 9 min) soundings is available for each group in table A 1, where it will be found, for example, that the average $\overline{W}$ for boat releases is lower by about 0·15 m/s than that for releases from P or Q. This is unlikely to be due to sampling variations. Thus on some days balloons were released from only one station under more or less identical weather conditions and successive groups of about 10 of these ascents yield values of $\overline{W}$ which agree to about 0·05 m/s which should be compared with the values of table A 1. Since there was no selection of balloons or variation in filling procedure according to release point in the primary series, the lower average value of $\overline{W}$ for boat releases strongly suggests the existence of an overall mean downward motion of the air in flights over the water relative to the overall mean vertical motion of the air in flights made from P or Q. There is also further evidence, of an indirect nature, that variations in $\overline{W}$ from group to group are at least partially indicative of variations in overall mean vertical motion of the air. Thus table A 1 shows that $\overline{w}$ is mainly negative in the lower levels of flights from the boat, but that, rather surprisingly, it reverses at higher levels while balloons are still well to seaward of the coast. This also suggests a systematic positive error in $\overline{w}$ for boat releases.

To obtain the appropriate correction to $\overline{w}$ for every group it is necessary to arrive at the best estimate of the rate of ascent of the balloons relative to the air and to subtract this from the value of $\overline{W}$ for each group. We have considered various methods of making the required estimate, e.g. by assuming the correction to $\overline{w}$ to be zero in groups composed of ascents made in high winds, or by reference to Ludlam (1953), but have decided that we cannot do better at the moment than assume the mean vertical motion over all soundings to be zero. The correction to $\overline{w}$ for any group is then given by the difference of $\overline{W}$ for this group from the value of $\overline{W}$ for all soundings, i.e. 49·5 m/20 s.

Downloaded from rsta.royalsocietypublishing.org

The mean vertical velocity of the air, a function of the spatial co-ordinates, and of the time, is presumably determined by appropriate mean values of the horizontal wind speed and direction, the field of radiation, and the lapse rate of virtual temperature upwind of the island. Our observations are not, however, sufficiently comprehensive to allow a detailed analysis in terms of all these variables, although the arrangement of table A 1 has been made with a number of them in mind (all ascents were made with the sun well above the horizon). The most effective method of presentation of the results is accordingly in some doubt and we have chosen to represent them in two ways:

(i) By means of plan trajectories (figure A 1) relative to the island, continuous lines being drawn where the mean motion is upward, discontinuous lines where it is downward, $\overline{w}$ in table A 1 having been corrected for the departure of $\overline{W}$ for each group from 49·5 m/20 s. It must, of course, be remembered that the trajectories are those of balloons and not of the air.

(ii) By graphs of $\overline{w}$, corrected and uncorrected, against height z for five combinations of groups having notably different trajectories from one combination to another (figure A 2); the zero of the abscissa is in each case appropriate to the corrected values of $\overline{w}$, the amount of the correction being shown by a suitably located mark on the abscissa. An ordinate drawn through this mark necessarily intersects the curve of $\overline{w}$ to give equal areas on either side. It is encouraging to note that the corrections applied to each group in a combination of groups turns out to be mainly of one sign.

Turning first to figure A 1, the mean vertical motion is seen to be initially upward for most groups with island release points P or Q, and that for these groups descent generally sets in at higher levels, roughly at, or somewhat beyond, the further coastline when the trajectories cross it. These features are not unreasonable, though it is to be remembered that the water on the downwind side of the island is rather shallow and so probably warm compared with the more distant sea—the island surface is, however, much the hotter during most of the period of the ascents. Descending motion is also apparent in higher levels for land release points when the balloons remain over the island. Whether this is or is not reasonable, it is consistent with the general absence of cumulus in these parts of the trajectories. At the highest levels sounded, a few groups for land release points show a reversal to upward mean motion over the sea as well as over the land. In this connexion it is to be noted that the Anegada cumulus (§ 5·1 and figure 4) commonly had its upwind end not far from the end-points of the trajectories for groups Q and V.

Three groups (D, G and M) show ascent only—evidence perhaps that the variance in the rate of ascent of balloons relative to the air or of the rate of ascent of the air itself is somewhat too great to allow corrections to $\overline{w}$ to be applied with confidence to groups of the size used. Upward vertical motion of the air throughout a balloon trajectory is not of course to be excluded, even if no cloud occurs at any point along it, for the balloon trajectories are not trajectories of the air—air found ascending towards the end of a trajectory such as for group D, in which there is little change of direction with height, may well be descending at points above the early part of the balloon trajectory. The correction to $\overline{w}$ for soundings with a boat release change substantially the pattern of $\overline{w}$ shown in table A 1. The mean motion is seen to be downward almost throughout the trajectories which are wholly over water with ascent at the beginning and end of two trajectories. The number of

Downloaded from rsta.royalsocietypublishing.org

ascents composing each group from the boat is, however, rather small, so that an average such as is given in figure A 2 (*a*) for three of these groups is probably needed to obtain more representative values. In this figure the increase of downward motion as the surface is

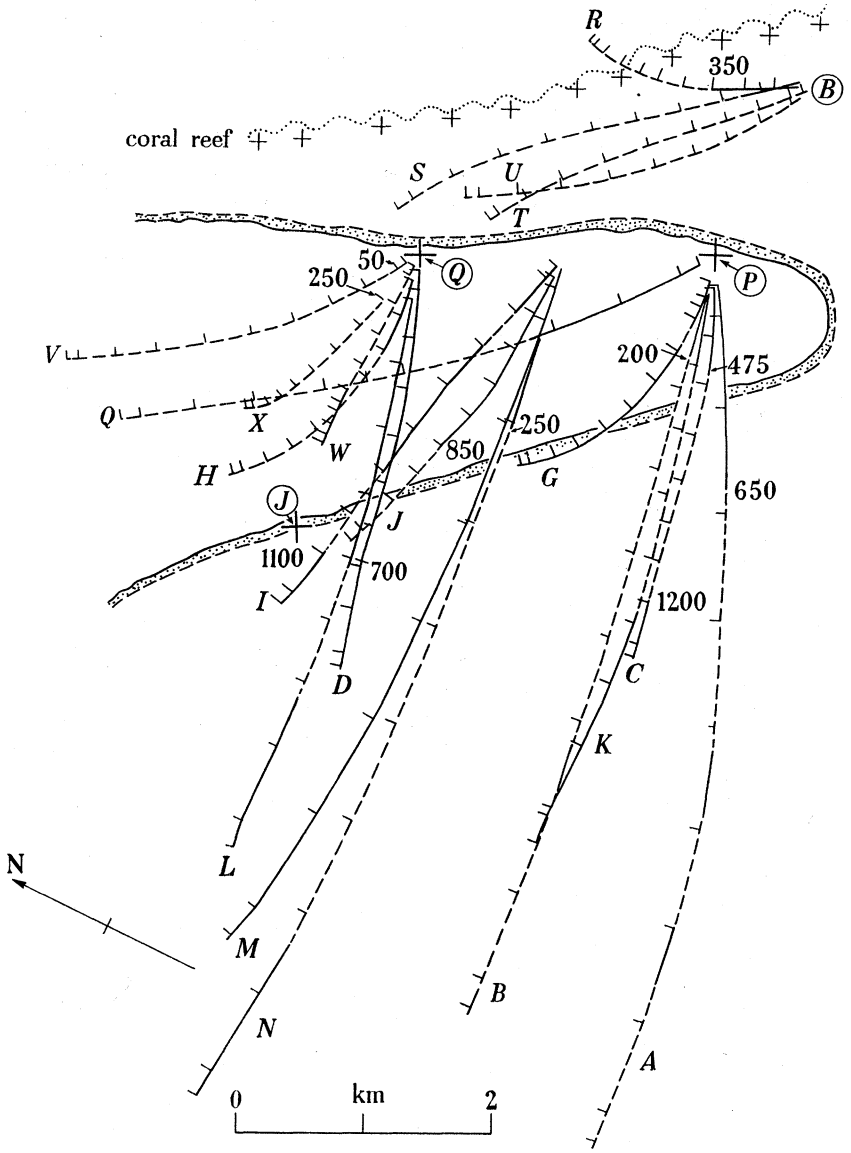

FIGURE A 1. Mean plan trajectories of balloons in groups defined in table 12. Four groups omitted for clarity. Groups which have balloons starting alternately from *P* and *Q* are plotted from mid-point of *PQ*. Ascending air shown by full lines, descending air by dotted lines, assuming that the rate of rise of balloons relative to the air is the mean rate of rise of the balloons over all soundings (49·5 m/20 s). Side marks on trajectories at heights 50, 100, 250, 400, 550, 700, 850, 1000, 1150, 1300 and 1350 m. Figures on trajectories show estimated height of change over from ascent to descent for some trajectories.

approached is due to an approximation used in determining the zero for height which only affects boat releases; otherwise the variation of vertical velocity with height carries conviction. There is only one apparently gross inconsistency in figure A 1, i.e. as between groups M and N. These groups refer to ascents made on the morning and afternoon respectively of the same day, the morning being cloudy and showery.

Downloaded from rsta.royalsocietypublishing.org

Groups S, T, U from the boat, Q from station P, and V from station Q provide a set of trajectories for not dissimilar winds, though group Q has higher winds than the others. Taken together they provide vertical cross-sections along the mean motion for winds only moderately inclined to the shore-line and imply descending motion aloft over the sea and land with ascending motion in the lower levels at, and immediately downwind of, the shore-line—this is a coherent pattern.

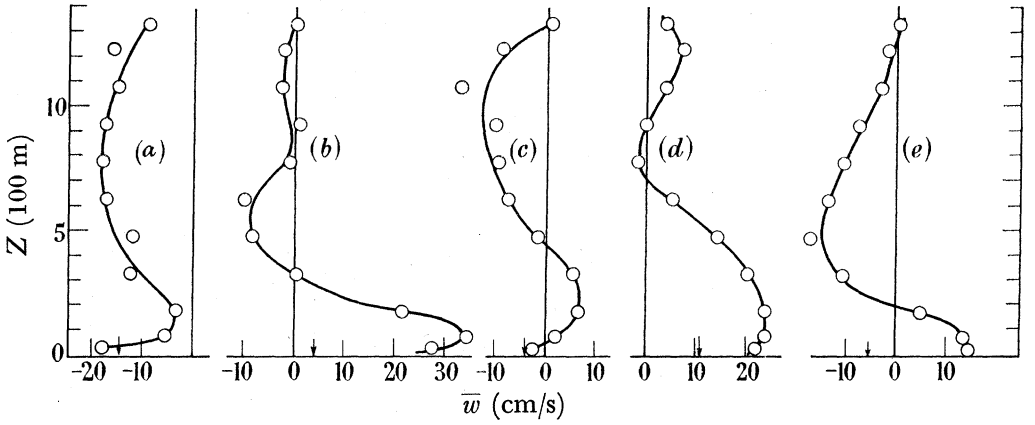

FIGURE A 2. Mean vertical profiles of vertical velocity of air assuming mean rate of ascent of balloon is $\overline{W} = 49{\cdot}5$ m/20 s. Arrows on abscissae show the corrections which have been applied (table A 1) for the difference of the mean rate of ascent for a group from 49·5 m/20 s. (*a*) Mean of groups S, T, U; from boat, 28 ascents, $U_0 = 4{\cdot}1$ m/s. (*b*) Mean of groups A, B, C, K; from P, 65 ascents, $U_0 = 9{\cdot}0$ m/s. (*c*) Group Q; from P, 12 ascents in 1 day, $U_0 = 8{\cdot}1$ m/s. (*d*) Mean of groups D, L; from Q, 31 ascents, $U_0 = 7{\cdot}3$ m/s. (*e*) Mean of groups H, V, W, X; from Q, 74 ascents, $U_0 = 4{\cdot}4$ m/s.

Groups G, H refer to ascents made alternately from stations P and Q on the same day. While the former group shows ascent throughout the trajectory the latter group shows descending motion above about 400 m. This difference, if genuine, indicates a substantial modification of the pattern of vertical motion in the downwind direction from the south-east extremity of the island. Groups K, L, also referring to ascents made alternately from P and Q, show, on the other hand, remarkably similar patterns of mean flow. For these two groups, however, the wind is practicaly normal to the shore-line and is a good deal stronger than in group G, H.

Groups M, N apart, there is no evidence for any material change in the pattern or intensity of vertical motion as between morning and afternoon ascents, e.g. groups E and F, I and J, W and X, although group F (p.m.) shows some intensification on group E (a.m.).

The magnitude of the vertical motion, as given in figure A 2, oscillates generally between about ± 20 cm/s and does not appear to exhibit any strong dependence on wind speed*—a notable result of which there can be little doubt. Such variation as does occur is perhaps in the sense of $\overline{w}$ increasing with wind speed, for among the individual groups of table A 1 we note that of groups A, B and C, which apart from wind speed are roughly comparable, groups A and B, made in high winds, have greater vertical velocities than group C made in a lighter wind. Similarly, group L, made in higher winds but otherwise comparable with group D, has the greater vertical velocities.

* The fluctuation analysis (§9) showed also that values of $\overline{w'^2}$ did not vary markedly with wind speed.

Downloaded from rsta.royalsocietypublishing.org

To summarize this part of the analysis of the island effect, it is evident that the technique of balloon observation adopted is capable of providing the mean vertical motion as a function of height and horizontal position, but that a more refined technique is required in order to ascribe with adequate precision the position of the origin of $\overline{w}$ in the $\overline{w}$-axis. This refinement of technique may well prove possible, but the labour of evaluating the field of $\overline{w}$ in a comprehensive fashion would indeed be formidable. For an island such as Anegada it is now reasonably established that the mean vertical motions outside cloud are of order 20 cm/s up to about 1·5 km.

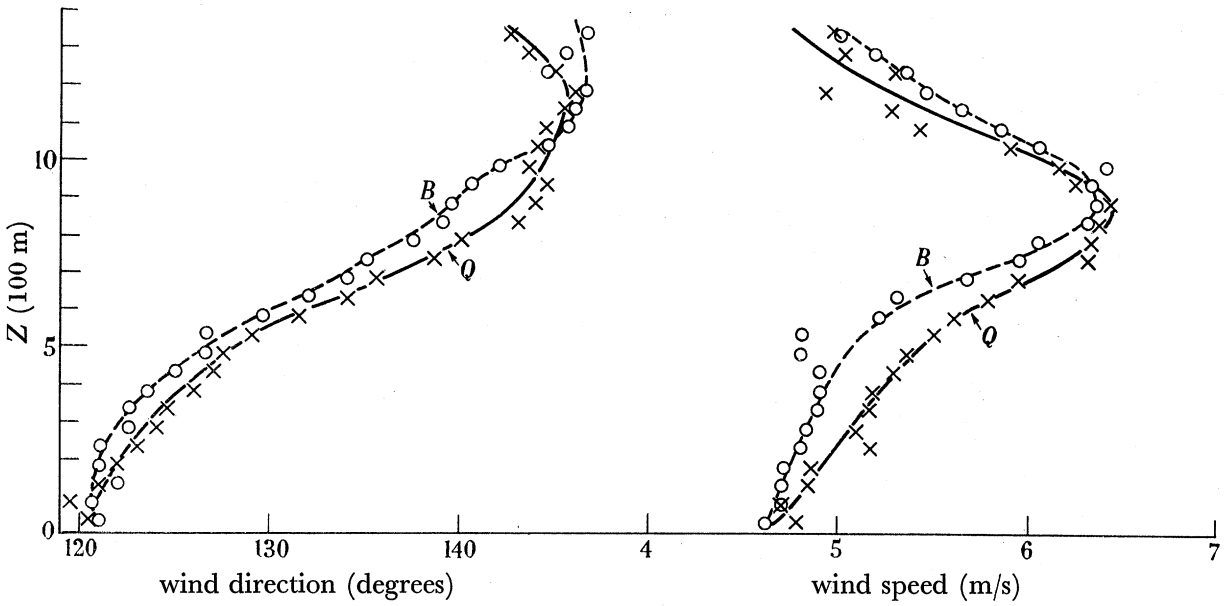

FIGURE A 3. Comparison between wind speed and direction profiles for ascents from boat (group U) and Q (group V) taken alternately throughout 4 April. ○, boat releases; ×, Q releases.

A 3. *The effect of the island on the field of horizontal motion*

The release of balloons from stations P, Q and B on the upwind side of the island and from station J on the downwind side (see § 3·4), the latter over periods when ascents were also being made from the upwind side, provides information on the adequacy of stations P, Q for sampling oceanic air—a major concern—and on sea breeze effects produced by the island. But the locations of stations P, Q, B and J (all well towards the south-east end of the island) are evidently not well designed for the latter investigation which was in any event incidental to the main programme.

The main results of this paper have been deduced from observations of balloons in the primary series and to investigate the adequacy of P, Q as release points, we will first examine the differences in the field of horizontal motion using P, Q and B as release points. On one day, 4 April, balloons were released alternately from stations B and Q (groups U and V of table A 1). Mean vertical profiles of wind speed and direction for the two groups are shown in figure A 3 (see also figure A1 for the corresponding trajectories). The difference in the two pairs of curves as drawn is small, at most 0·3 m/s in speed and 4° in direction, and generally appreciably less. The turning point in the speed profile is practically the same for both groups within the accuracy of drawing. Since the differences between

Downloaded from rsta.royalsocietypublishing.org

the two pairs of profiles are mainly systematic it is not unlikely that the island is responsible, though a comparison of alternate ascents made from one station Q indicates that differences of the same order as those shown in figure A 3 could arise from sampling. Moreover, the boat profiles are ascribed to somewhat too great a height relative to the Q profiles because of the different mean rates of ascent in the two groups (not allowed for in figure A 3), so that the differences are not quite so large as appear. If we take the differences to be real and the mean difference in speed up to 800 m to be 0·2 m/s, the horizontal divergence over the 3·4 km path from B to Q corresponds in a two-dimensional field to a vertical convergence of 5 cm/s over the 800 m layer. The results of the previous section

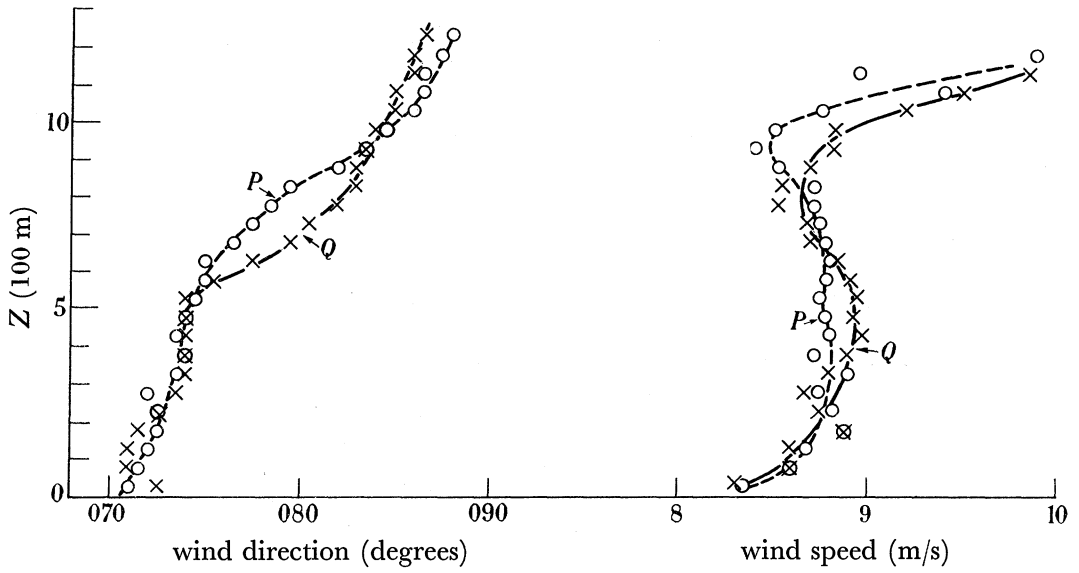

FIGURE A 4. Comparison between wind speed and direction profiles for ascents from P (group K) and Q (group L) taken alternately throughout 23 March. ○, P releases; ×, Q releases.

(figure A 2) show that an increase in the velocity of descent of about this amount is very plausible, and the difference of speed shown in figure A 3 is therefore probably significant. The differences in the direction profiles, essentially a small veer of the wind over the land relative to the wind over the sea, is possibly a reflexion of the horizontal convergence of streamlines at the downwind end of the heated island—increasing surface friction at the island would of itself lead to a contrary difference.

We have no *a priori* evidence that ascents from the boat are completely typical of the oceanic air, but the small difference between the B and Q ascents just examined suggests that those from B should hardly be measurably different from those a little more to windward. Further, the comparison between B and Q was made on a day of rather light wind when differences, in direction at least, might be expected to be most in evidence. The difference in direction is in the sense of leading to a slight underestimate of τ_0 by the method of geostrophic departures used in § 7. It should have no significant consequence for the analysis of fluctuations given in § 9.

Continuing the analysis of ascents made from the upwind side of the island, figures A 4, 5 show wind speed and direction profiles for daily groups relating to P and Q as release points, the ascents alternating as before between the two stations. Figure A 4, for groups K and L,

Downloaded from rsta.royalsocietypublishing.org

refers to a fresh wind practically normal to the coastline whereas figure A 5, for groups G and H, refers to a lighter wind with rather small inclination to the coastline. No systematic differences can be seen in the profiles of figure A 4 in the lower levels, and such differences as appear aloft may perhaps be due to inhomogeneity of data—it would be unlikely for the site of release to influence the upper levels and not the lower. Groups G and H have been referred to already in the previous section of the Appendix as showing essentially the same pattern of mean vertical motion. In figure A 5, however, systematic differences in the profiles do appear, particularly for direction; *P* ascents are veered on *Q* ascents both at lower and upper levels, and there is a suggestion that the speeds from *P* are higher below

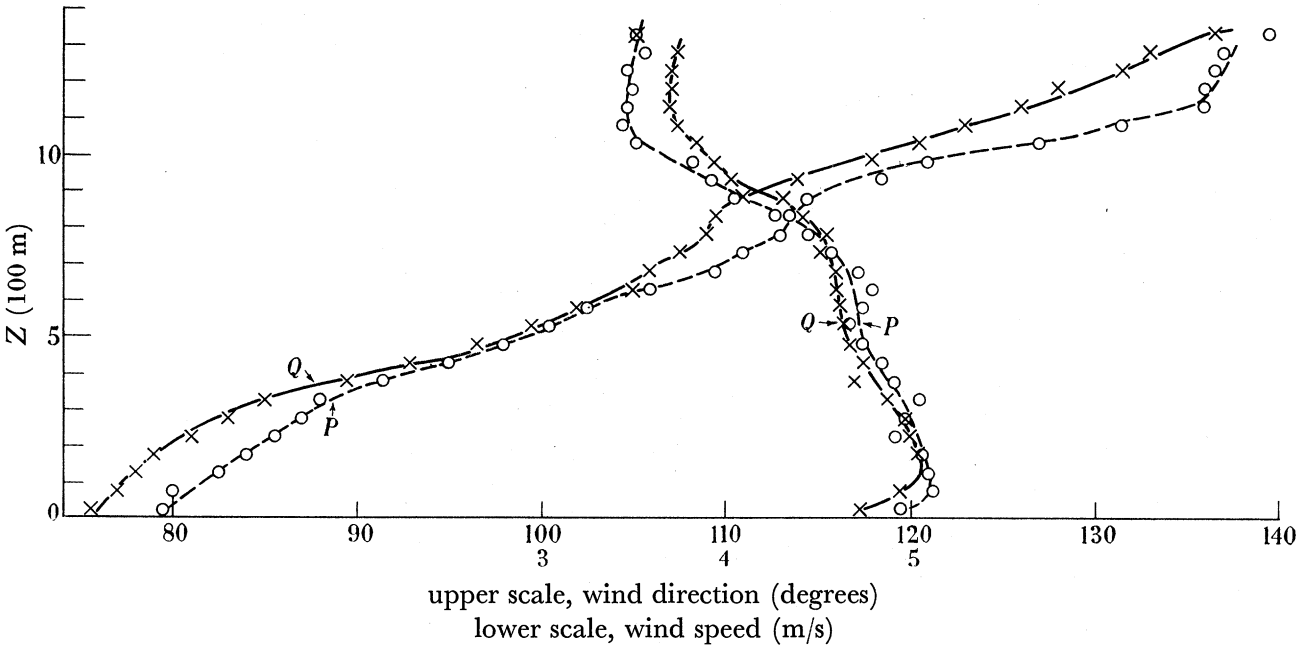

FIGURE A 5. Comparison between wind speed and direction profiles for ascents from *P* (group G) and *Q* (group H) taken alternately throughout 19 March. ○, *P* releases; ×, *Q* releases.

and less aloft than those from *Q*. Again, the differences might arise from sampling, but a difference in the pattern of vertical motion for these two groups has already been noted in the previous section. The difference in direction between *P* and *Q* ascents is consistent with the convergence of streamlines already suggested by the *B*, *Q* comparison above for the south-east end of the island, but it is perhaps surprising to find the difference present aloft. The difference of direction of about 4° up to 300 m or so, over which layer there is no marked difference in speed, provides a horizontal convergence which would be consistent with a vertical divergence of about 5 cm/s over the layer. In both groups of soundings there was ascent over the layer with vertical velocities at 300 m of about this magnitude.

There is therefore some evidence that the island produces small differences in the winds from *P* and *Q* releases in light winds, but these differences are probably too small and not sufficiently consistent in the primary series as a whole to affect significantly the analysis of the mean motion and the fluctuations in §§ 6 to 9.

We turn now to the ascents of the secondary series from stations *J* and *Q* (see §§ 3·4 and 4·2) which, in combination with the relevant ascents of the primary series, give a larger-

Downloaded from rsta.royalsocietypublishing.org

scale picture of the effect of the island on the horizontal motion of the air. The ascents made between 0930 and 1630 l.m.t., that is, over about the same period to which the previous results and analysis apply, will be considered first.

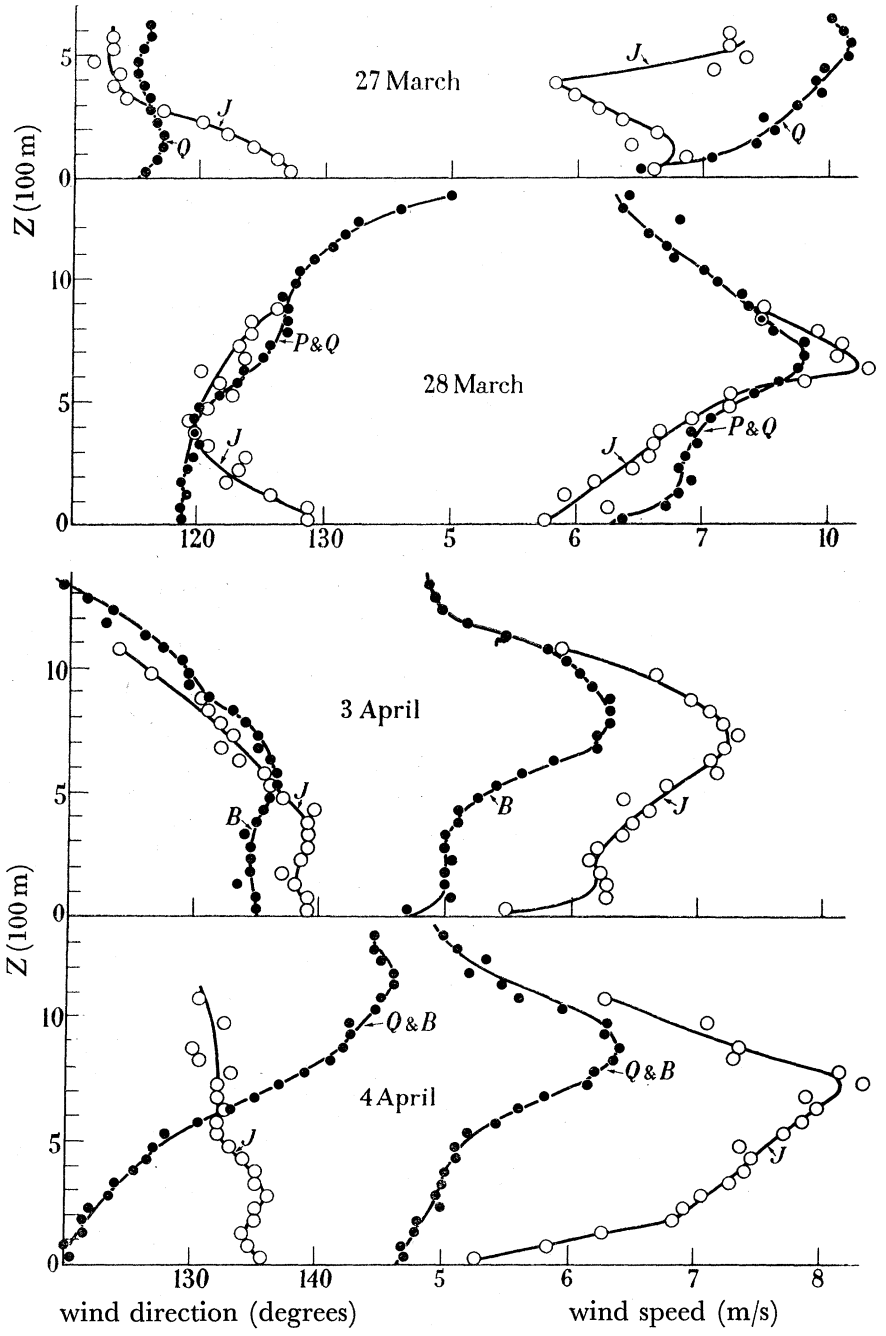

FIGURE A 6. Daily mean profiles (0930 to 1630) of wind speed and direction for ascents on upwind (P, Q or B) and downwind (J) sides of island. J ascents are all made with single theodolite observations. ○; J releases, ●; P, Q and B releases.

Figure A 6 shows the mean vertical profiles of wind speed and direction for ascents made on either side of the island on 4 days. All ascents from station J were made using a single theodolite, a rate of ascent of 2·5 m/s being assumed. Those from Q on 27 March were also

Downloaded from rsta.royalsocietypublishing.org

single theodolite ascents, worked up similarly. Further, all the ascents on 27 March were terminated at minute 5 from release in order to obtain more frequent soundings—balloons were released at 6 min intervals for 30 min during every hour. The mean surface wind direction for the 4 days was about the same (from 115 to 135° at the north-east side of the island) and the mean surface wind speed also changed rather little (from 4·7 m/s to 6·5 m/s at the north-east side of the island). All four pairs of direction profiles in figure A 6 show some common features, namely, in the lower layers a veer of the wind at *J* relative to that on the other side of the island and in the upper layers a back. The differences in direction are most marked on 4 April, the day of lightest surface wind, with 14° difference at the surface and about the same but of opposite sense at 1 km. Thus clear evidence is provided of convergence of streamlines on the south-east end of the island in the lower layers, up to 300 or 500 m, and of divergence at higher levels, but farther downwind. The profiles of wind speed are not so clearly differentiated on the two sides of the island. On 3 and 4 April there is a notably similar differentiation, station *J* having much stronger wind except at the surface and aloft, in spite of very dissimilar variations of direction with height on the north-east side of the island on the 2 days. This difference in speed is, however, reversed on 27 March and, for the lower layers, on 28 March also. 27 March is exceptional in showing a speed profile at *J* of entirely different shape from all the rest. The maximum wind speed at a few hundred metres, characteristic of the Trades, is present on the other days, though on 3 and 4 April it is somewhat higher at *J* than on the north-east side of the island, perhaps due to a greater mean rate of ascent of balloons released from station *J*.

Ascents made on 27 March before and after the normal observing period, namely, between 0730 and 0930, and between 1630 and 1830, failed to provide any clear evidence of a diurnal variation in the distortion of the field of horizontal motion by the island.

References

Charnock, H. & Robinson, G. D. 1956 *Quart. J. R. Met. Soc.* (submitted for publication).

Deacon, E. L. 1955 The turbulent transfer of momentum in the lowest layers of the atmosphere. *Met. Phys. Tech. Pap.* no. 4, C.S.I.R.O., Australia.

Dryden, H. L. 1948 *Advances in applied mechanics*, **1**, 2. New York: Academic Press.

Durst, C. S. 1954 Variation of wind with time and distance. *Geophys. Mem., Lond.*, no. 93.

Ellison, T. H. 1956 *Surveys in mechanics* (ed. Batchelor and Davies), p. 400, Atmospheric turbulence. Cambridge University Press.

Estoque, M. A. 1955 The spectrum of large scale turbulent transfer of momentum and heat. *Tellus*, **7**, 177.

Ludlam, F. H. 1953 The rate of rise of pilot balloons. *Met. Mag.* **82**, 306.

Malkus, J. S. & Ronne, C. 1954 On the structure of some cumulonimbus clouds which penetrated the high tropical troposphere. *Tellus*, **6**, 351.

Malkus, J. S. & Stern, M. E. 1953 The flow of a stable atmosphere over a heated island. Part I. *J. Met.* **10**, 30.

Meteorological Office 1948 *Monthly weather charts of the Atlantic Ocean*, M.O. 483.

Priestley, C. H. B. 1949 Heat transport and zonal stress between latitudes. *Quart. J. R. Met. Soc.* **75**, 28.

Riehl, H., Yeh, T. C., Malkus, J. S. & La Seur, N. E. 1951 The North-East Trade of the Pacific Ocean. *Quart. J. R. Met. Soc.* **77**, 598.

PHILOSOPHICAL TRANSACTIONS OF THE ROYAL SOCIETY A MATHEMATICAL, PHYSICAL & ENGINEERING SCIENCES

PHILOSOPHICAL TRANSACTIONS OF THE ROYAL SOCIETY A MATHEMATICAL, PHYSICAL & ENGINEERING SCIENCES

Downloaded from rsta.royalsocietypublishing.org

Sheppard, P. A. 1953 Momentum flux and meridional motion in the general circulation. *Proc. Toronto Met. Conf. R. Met. Soc.* p. 103.

Sheppard, P. A. 1954 The vertical transfer of momentum in the general circulation. *Arch. Met., Wien*, A, **7**, 114.

Sheppard, P. A., Charnock, H. & Francis, J. R. D. 1952 Observation of the westerlies over the sea. *Quart. J. R. Met. Soc.* **78**, 563.

Sheppard, P. A. & Omar, M. H. 1952 The wind stress over the ocean from observations in the Trades. *Quart. J. R. Met. Soc.* **78**, 583.

Smith, R. C. 1955 Theory of airflow over a heated land mass. *Quart. J. R. Met. Soc.* **81**, 382.

Starr, V. P. & White, R. M. 1952 Two years of momentum flux data for 31°N. *Tellus*, **4**, 332.

Starr, V. P. & White, R. M. 1954 Two years of momentum flux data for 13°N. *Tellus*, **6**, 180.

Sutcliffe, R. C. 1936 Surface resistance in atmospheric flow. *Quart. J. R. Met. Soc.* **62**, 3.

Swinbank, W. C. 1955 An experimental study of eddy transports in the lower atmosphere. *Met. Phys. Tech. Pap.* no. 2, C.S.I.R.O., Australia.

U.S. Weather Bureau 1952 *Normal weather maps of the northern hemisphere. Tech. Pap.* 21.

PHILOSOPHICAL TRANSACTIONS OF THE ROYAL SOCIETY A MATHEMATICAL, PHYSICAL & ENGINEERING SCIENCES

PHILOSOPHICAL TRANSACTIONS OF THE ROYAL SOCIETY A MATHEMATICAL, PHYSICAL & ENGINEERING SCIENCES

PHILOSOPHICAL TRANSACTIONS OF THE ROYAL SOCIETY A MATHEMATICAL, PHYSICAL & ENGINEERING SCIENCES

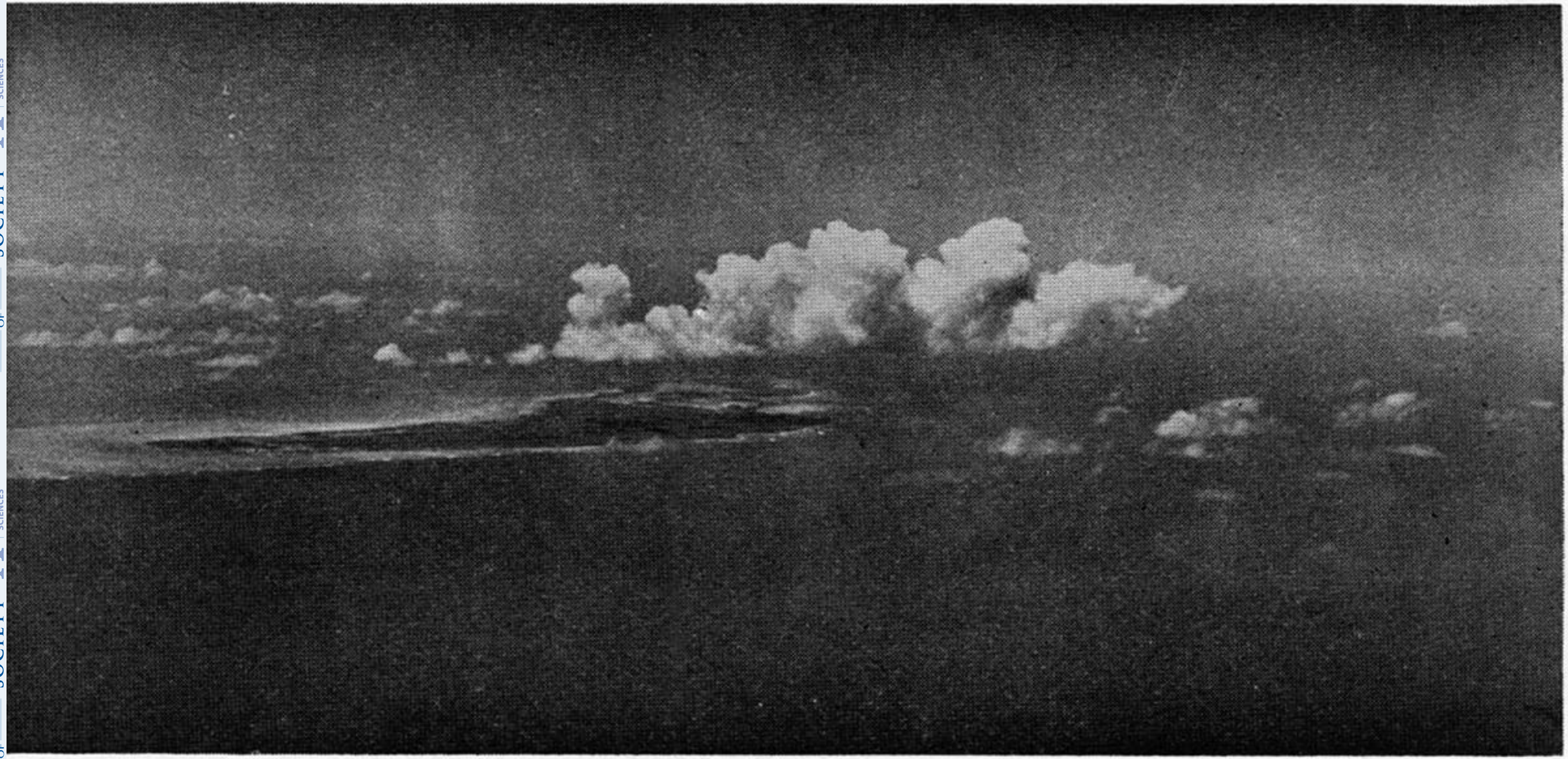

FIGURE 4. Aerial photograph of Anegada showing the island cumulus, the ring of nearly clear air around, and the Trade cumuli surrounding all. Photograph by K. McCasland.

PHILOSOPHICAL TRANSACTIONS OF THE ROYAL SOCIETY A MATHEMATICAL, PHYSICAL & ENGINEERING SCIENCES